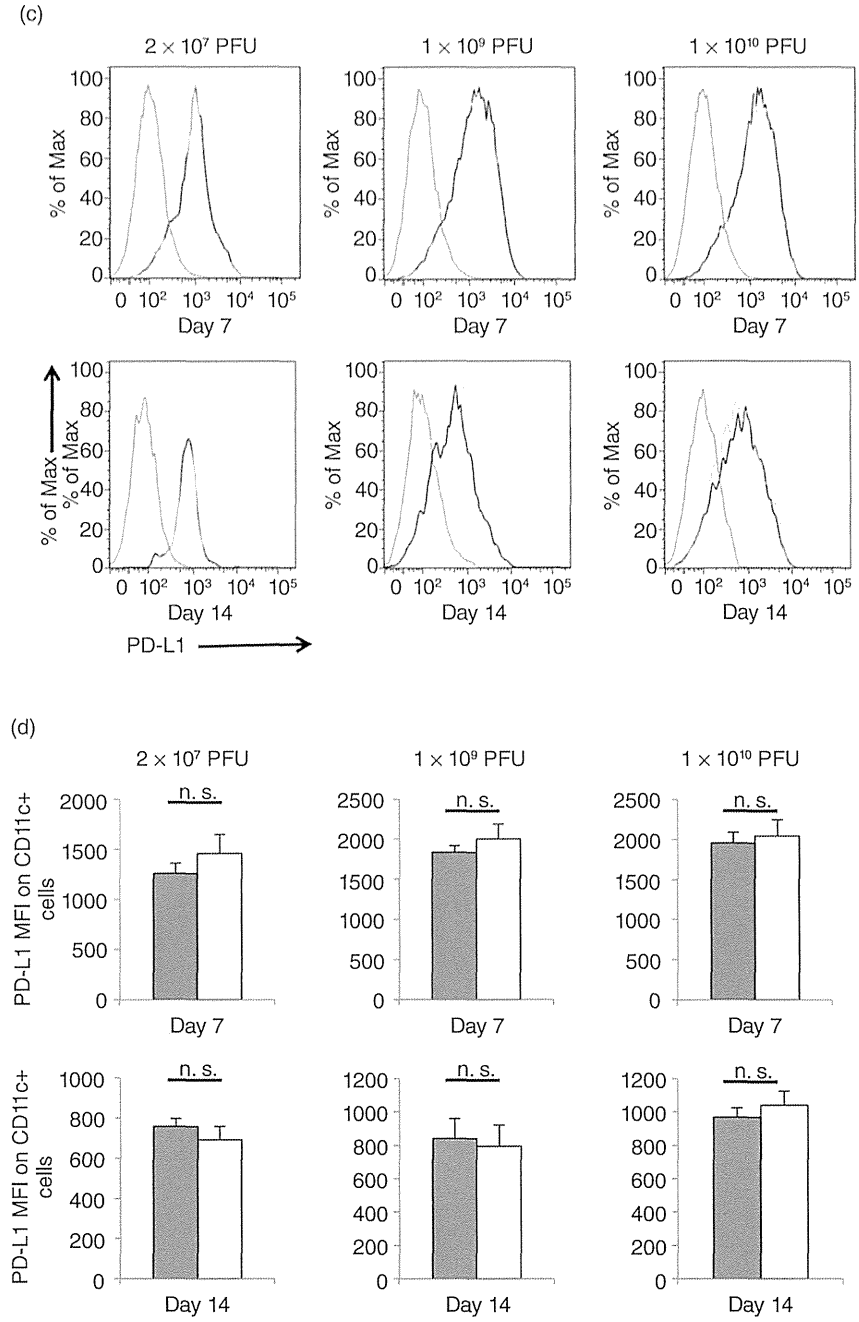

Figure 5 *Continued*

extensive investigations of inhibitory receptors in the regulation of T cells in human chronic viral infections.[25,26]

Chronic HCV infection in humans is characterized by CD8 T-cell exhaustion and dysfunction.[27] As in chronic LCMV infection, the expression of PD-1 is similarly upregulated on the virus-specific CD8 T cells in chronic HCV infection, and HCV-specific PD-1^{high} T cells are functionally impaired.[28–30] Also, Tim-3 is overexpressed on HCV-specific dysfunctional CD8 T cells.[25] In addition, a blockade of PD-1/PD-L1 or Tim-3/galectin9 (Gal9) interaction restores T-cell functions such as proliferation, cytolytic activity and cytokine (IFN-γ and tumor necrosis factor-α) production.[25,28–30] As was

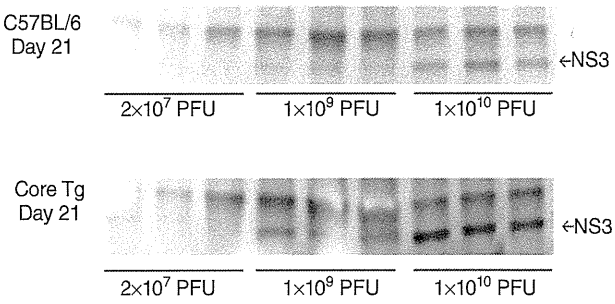

Figure 6 Persisting hepatitis C virus (HCV)-NS3 antigen detection was performed on the liver sections isolated 21 days post-infection. Liver sections were analyzed by IP-western blot assay using anti-FLAG antibody.

mentioned above, it has been reported that increased expression of inhibitory receptors is associated with the impaired HCV-specific CD8 T cells observed in chronic HCV patients. However, the underlying mechanisms for HCV-mediated impaired CD8 T-cell responses have yet to be determined. Based on our finding that lower level of activation and higher levels of expression of regulatory molecules, Tim-3 and PD-1, by intrahepatic CD8 T cells and higher levels of expression of PD-L1 by intrahepatic APC were observed in core (+) mice in comparison with core (−) mice, it is possible that HCV core-induced T-cell dysfunction is one of the viral factors that contributes to impaired CD8 T-cell responses as seen in chronic HCV patients. Our speculation is in accordance with the study by Lukens *et al.*[31]

Suppression of CTL responses via highly expressed Ag was found in chronic HCV infection. Inverse relationships between HCV viral titer and HCV-specific T cells have been reported.[7,32,33] In this study, we found higher levels of expressions of PD-L1 by intrahepatic APC and an impaired intrahepatic CD8 T-cell response in high infectious dose setting. Moreover, we found a significant inverse correlation between the percentages of IFN-γ-producing cells and expression of regulatory molecules in Ag-specific intrahepatic CD8 T cells. It is likely that the PD-1/PD-L1 or Tim-3/Gal9 pathway play a major inhibitory role in our model. High-dose Ad-HCV NS3 infection may inhibit the NS3-specific CD8 T-cell responses not at the induction phase but at the effector phase because Ag-specific-MHC tetramer$^+$ T cells were observed, and most Ag-specific MHC tetramer$^+$ T cells was anergic to PMA/ionophore stimulation and these T cells expressed PD-1 and Tim-3. The role of PD-1/PD-L1 as mechanism for liver tolerance has been well established. PD-1 expression by T cells has been shown to inhibit intrahepatic antiviral immune responses at the effector phase.[34–36]

Hepatitis C virus infection affects approximately 170 million people in the world and is a major global health problem because infected individuals can develop liver cirrhosis and hepatocellular carcinoma. Pegylated interferon and ribavirin therapy, although beneficial in approximately half of treated patients, are expensive and associated with significant side-effects.[37] In this clinical context, there is an urgent need for the development of a therapeutic and/or prophylactic HCV vaccine.[38] Because HCV infects only humans and chimpanzees, it is difficult to evaluate effective therapeutic vaccine candidates. Recently, as a small animal model for HCV infection study, chimeric humanized mouse harboring a human hepatocyte and hematolymphoid system was established by xenotransplantation technique.[39,40] The xenograft model provides a unique opportunity for HCV vaccine development. However, the generation of this chimeric humanized mouse requires advanced technical skills and the scarcity of adequate human primary material remains a significant logistical challenge.[41,42] Our model showed in the present study is easy to create, and it has Ag-specific T-cell exhaustion and Ag persistent in the liver seen in chronic HCV patients. These features suggest that this system is useful for therapeutic HCV vaccine development.

ACKNOWLEDGMENTS

THIS WORK WAS supported by grants from a Saitama Medical University Internal Grant (24-A-1-01 and 24-B-1-06), Grant from Ochiai Memorial Award 2011 and the Ministry of Health, Labor, and Welfare, Japan. The authors thank Hiroe Akatsuka for technical assistance.

REFERENCES

1 Shepard CW, Finelli L, Alter MJ. Global epidemiology of hepatitis C virus infection. *Lancet Infect Dis* 2005; **5**: 558–67.
2 Kamal SM. Acute hepatitis C: a systematic review. *Am J Gastroenterol* 2008; **103**: 1283–97.
3 Alter HJ, Seeff LB. Recovery, persistence, and sequelae in hepatitis C virus infection: a perspective on long-term outcome. *Semin Liver Dis* 2000; **20**: 17–35.
4 Grüner NH, Gerlach TJ, Jung MC *et al.* Association of hepatitis C virus-specific CD8+ T cells with viral clearance in acute hepatitis C. *J Infect Dis* 2000; **181**: 1528–36.

5 Chang KM, Rehermann B, McHutchison JG *et al.* Immunological significance of cytotoxic T lymphocyte epitope variants in subjects chronically infected by the hepatitis C virus. *J Clin Invest* 1997; **100**: 2376–85.
6 Lechmann M, Woitas RP, Langhans B *et al.* Decreased frequency of HCV core-specific peripheral blood mononuclear cells with type 1 cytokine secretion in chronic hepatitis. *Can J Hepatol* 1999; **31**: 971–8.
7 Rehermann B, Chang KM, McHutchison JG *et al.* Differential cytotoxic T-lymphocyte responsiveness to the hepatitis B and C viruses in chronically infected patients. *J Virol* 1996; **70**: 7092–102.
8 Wedemeyer H, He XS, Nascimbeni M *et al.* Impaired effector function of hepatitis C virus specific CD8+ T cells in chronic hepatitis C virus infection. *J Immunol* 2002; **169**: 3447–58.
9 Zinkernagel RM, Hengartner H. Regulation of the immune response by antigen. *Science* 2001; **293**: 251–3.
10 Moskophidis D, Lechner F, Pircher H, Zinkernagel RM. Virus persistence in acutely infected immunocompetent mice by exhaustion of antiviral cytotoxic effector T cells. *Nature* 1993; **362**: 758–61.
11 Wherry EJ, Blattman JN, Murali-Krishna K, van der Most R, Ahmed R. Viral persistence alters CD8 T-cell immunodominance and tissue distribution and results in distinct stages of functional impairment. *J Virol* 2003; **77**: 4911–27.
12 Zajac AJ, Blattman JN, Murali-Krishna K *et al.* Viral immune evasion due to persistence of activated T cells without effector function. *J Exp Med* 1998; **188**: 2205–13.
13 Wherry EJ, McElhaugh MJ, Eisenlohr LC. Generation of CD8 T cell memory in response to low, high, and excessive levels of epitope. *J Immunol* 2002; **168**: 4455–61.
14 Eisen-Vandervelde AL, Waggoner SN, Yao ZQ, Cale EM, Hahn CS, Hahn YS. Hepatitis C virus core selectively suppresses interleukin-12 synthesis in human macrophages by interfering with AP-1 activation. *J Biol Chem* 2004; **279**: 43479–86.
15 Watanabe T, Bertoletti A, Tanoto TA. PD1/PD-L1 pathway and T-cell exhaustion in chronic hepatitis virus infection. *J Viral Hepat* 2010; **17**: 453–8.
16 Yao ZQ, Eisen-Vanderveld A, Waggoner SN, Cale EM, Hahn YS. Direct binding of hepatitis C virus core to gC1qR on CD4+ and CD8+ T cells leads to impaired activation of Lck and Akt. *J Virol* 2004; **78**: 6409–19.
17 Yao ZQ, Nguyen DT, Hiotellis AI, Hahn YS. Hepatitis C virus core protein inhibits human T lymphocyte responses by a complement-dependent regulatory pathway. *J Immunol* 2001; **167**: 5264–72.
18 Cavanaugh VL, Guidotti LG, Chisari FV. Inhibition of hepatitis B virus replication during adenovirus and cytomegalovirus infections in transgenic mice. *J Virol* 1998; **72**: 2630–7.
19 von Freyend MJ, Untergasser A, Arzberger S *et al.* Sequential control of hepatitis B virus in a mouse model of acute, self-resolving hepatitis B. *J Viral Hepat* 2011; **18**: 216–26.
20 Moriya K, Yotsuyanagi H, Shintani Y *et al.* Hepatitis C virus core protein induces hepatic steatosis in transgenic mice. *J Gen Virol* 1997; **78**: 1527–31.
21 Koike K, Moriya K, Ishibashi K *et al.* Sialadenitis histologically resembling Sjogren syndrome in mice transgenic for hepatitis C virus envelope genes. *Proc Natl Acad Sci U S A* 1997; **94**: 233–6.
22 Kolykhalov AA, Agapov EV, Blight KJ, Mihalik K, Feinstone SM, Rice CM. Transmission of hepatitis C by intrahepatic inoculation with transcribed RNA. *Science* 1997; **277**: 570–4.
23 Frelin L, Alheim M, Chen A *et al.* Low dose and gene gun immunization with a hepatitis C virus nonstructural (NS) 3 DNA-based vaccine containing NS4A inhibit NS3/4A-expressing tumors in vivo. *Gene Ther* 2003; **10**: 686–99.
24 Barber DL, Wherry EJ, Masopust D *et al.* Restoring function in exhausted CD8 T cells during chronic viral infection. *Nature* 2006; **439**: 682–7.
25 Golden-Mason L, Palmer BE, Kassam N *et al.* Negative immune regulator Tim-3 is overexpressed on T cells in hepatitis C virus infection and its blockade rescues dysfunctional CD4+ and CD8+ T cells. *J Virol* 2009; **83**: 9122–30.
26 Sharpe AH, Wherry EJ, Ahmed R, Freeman GJ. The function of programmed cell death 1 and its ligands in regulating autoimmunity and infection. *Nat Immunol* 2007; **8**: 239–45.
27 Spangenberg HC, Viazov S, Kersting N *et al.* Intrahepatic CD8+ T-cell failure during chronic hepatitis C virus infection. *Hepatology* 2005; **42**: 828–37.
28 Golden-Manson L, Palmer B, Klarquist J, Mengshol JA, Castelblanco N, Rosen HR. Upreglation of PD-1 expression on circulating and intrahepatic hepatitis C virus-specific CD8+ T cells associated with reversible immune dysfunction. *J Virol* 2007; **81**: 9249–58.
29 Penna A, Pilli M, Zerbini A *et al.* Dysfunction and functional restoration of HCV-specific CD8 responses in chronic hepatitis C virus infection. *Hepatology* 2007; **45**: 588–601.
30 Radziewicz H, Ibegbu CC, Fernandez ML *et al.* Liver-infiltrating lymphocytes in chronic human hepatitis C virus infection display an exhausted phenotype with high levels of PD-1 and low levels of CD127 expression. *J Virol* 2007; **81**: 2545–53.
31 Lukens JR, Cruise MW, Lassen MG, Hahn YS. Blockade of PD-1/B7-H1 interaction restores effector CD8+ T cell responses in a hepatitis C virus core murine model. *J Immunol* 2008; **180**: 4875–84.
32 Sreekumar R, Gonzalez-Koch A, Maor-Kendler Y *et al.* Early identification of recipient with progressive histologic recurrence of hepatitis C after liver transplantation. *Hepatology* 2000; **32**: 1125–30.

33 Sugimoto K, Ikeda F, Standanlick J, Frederick A, Alter HJ, Chang KM. Suppression of HCV-specific T cells without differential hierarchy demonstrated ex vivo in persistent HCV infection. *Hepatology* 2003; **38:** 1437–48.
34 Isogawa M, Furuichi Y, Chisaki FV. Oscillating CD8+ T cell effector functions after antigen recognition in the liver. *Immunity* 2005; **23:** 53–63.
35 Iwai Y, Terawaki S, Ikegawa M, Okazaki T, Honjo T. PD-1 inhibits antiviral immunity at the effector phase in the liver. *J Exp Med* 2003; **198:** 39–50.
36 Maier H, Isogawa M, Freeman GJ, Chisari FV. PD-1:PD-L1 interactions contribute to the functional suppression of virus-specific CD8+ T lymphocytes in the liver. *J Immunol* 2007; **178:** 2714–20.
37 Pawlotsky JM. Therapy of hepatitis C: from empiricism to eradication. *Hepatology* 2006; **43:** S207–20.
38 Callendret B, Walker C. A siege of hepatitis: immune boost for viral hepatitis. *Nature Med* 2011; **17:** 252–3.
39 Legrand N, Ploss A, Balling R *et al.* Humanized mice for modeling human infectious disease: challenges, progress, and outlook. *Cell Host Microb* 2009; **6:** 5–9.
40 Robinet E, Baumert TF. A first step towards a mouse model for hepatitis C virus infection containing a human immune system. *J Hepatol* 2011; **55:** 718–20.
41 Kimura K, Kohara M. An experimental mouse model for hepatitis C virus. *Exp Anim* 2011; **60:** 93–100.
42 Ploss A, Rice CM. Towards a small animal model for hepatitis C. *EMBO Rep* 2009; **10:** 1220–7.

IJC
International Journal of Cancer

High ubiquitous mitochondrial creatine kinase expression in hepatocellular carcinoma denotes a poor prognosis with highly malignant potential

Baasanjav Uranbileg[1]*, Kenichiro Enooku[1,2]*, Yoko Soroida[1], Ryunosuke Ohkawa[1], Yotaro Kudo[2], Hayato Nakagawa[2], Ryosuke Tateishi[2], Haruhiko Yoshida[2], Seiko Shinzawa[2], Kyoji Moriya[3], Natsuko Ohtomo[2], Takako Nishikawa[2], Yukiko Inoue[2], Tomoaki Tomiya[2], Soichi Kojima[4], Tomokazu Matsuura[5], Kazuhiko Koike[2], Yutaka Yatomi[1] and Hitoshi Ikeda[1,2]

[1] Department of Clinical Laboratory Medicine, Graduate School of Medicine, The University of Tokyo, Tokyo, Japan
[2] Department of Gastroenterology, Graduate School of Medicine, The University of Tokyo, Tokyo, Japan
[3] Department of Infection Control and Prevention, Graduate School of Medicine, The University of Tokyo, Tokyo, Japan
[4] Micro-signaling Regulation Technology Unit, RIKEN Center for Life Science Technologies, Wako, Saitama, Japan
[5] Department of Laboratory Medicine, The Jikei University School of Medicine, Tokyo, Japan

We previously reported the increased serum mitochondrial creatine kinase (MtCK) activity in patients with hepatocellular carcinoma (HCC), mostly due to the increase in ubiquitous MtCK (uMtCK), and high uMtCK mRNA expression in HCC cell lines. We explored the mechanism(s) and the relevance of high uMtCK expression in HCC. In hepatitis C virus core gene transgenic mice, known to lose mitochondrial integrity in liver and subsequently develop HCC, uMtCK mRNA and protein levels were increased in HCC tissues but not in non-tumorous liver tissues. Transient overexpression of ankyrin repeat and suppressor of cytokine signaling box protein 9 (ASB9) reduced uMtCK protein levels in HCC cells, suggesting that increased uMtCK levels in HCC cells may be caused by increased gene expression and decreased protein degradation due to reduced ASB9 expression. The reduction of uMtCK expression by siRNA led to increased cell death, and reduced proliferation, migration and invasion in HCC cell lines. Then, consecutive 105 HCC patients, who underwent radiofrequency ablation with curative intent, were enrolled to analyze their prognosis. The patients with serum MtCK activity >19.4 U/L prior to the treatment had significantly shorter survival time than those with serum MtCK activity ≤19.4 U/L, where higher serum MtCK activity was retained as an independent risk for HCC-related death on multivariate analysis. In conclusion, high uMtCK expression in HCC may be caused by hepatocarcinogenesis *per se* but not by loss of mitochondrial integrity, of which ASB9 could be a negative regulator, and associated with highly malignant potential to suggest a poor prognosis.

Key words: ubiquitous mitochondrial creatine kinase, ankyrin repeat and suppressor of cytokine signaling box protein 9, hepatocellular carcinoma, prognostic factor

Abbreviations: AFP: alpha-fetoprotein; ALT: alanine aminotransferase; ASB: ankyrin repeat and suppressor of cytokine signaling box protein; AST: aspartate aminotransferase; DCP: des-gamma-carboxy prothrombin; GGT: gamma-glutamyltransferase; HCC: hepatocellular carcinoma; HCV: hepatitis C virus; RFA: radiofrequency ablation; ROC: receiver operating characteristic; SOCS: suppressor of cytokine signaling; uMtCK: ubiquitous mitochondrial creatine kinase

*B.U. and K.E. contributed equally to this work

DOI: 10.1002/ijc.28547

History: Received 2 July 2013; Accepted 1 Oct 2013; Online 15 Oct 2013

Correspondence to: Hitoshi Ikeda, Department of Clinical Laboratory Medicine, Graduate School of Medicine, The University of Tokyo, 7-3-1 Hongo, Bunkyo-ku, Tokyo 113-8655, Japan, Tel.: +81-3-3815-5411, Fax: +81-3-5689-0495, E-mail: ikeda-1im@h.u-tokyo.ac.jp

Primary liver cancer, 95% of which is hepatocellular carcinoma (HCC), is ranked third in men and fifth in women as a cause of death from malignant neoplasms in Japan.[1] Furthermore, the worldwide incidence of HCC has increased over several decades, and HCC has recently received considerable attention as a common cause of mortality.[2] HCC often arises in background of liver cirrhosis, which is formed as a result of chronic viral infections, alcoholic injury and some other disorders in the liver.[3,4] Of note, HCC has recently been linked to non-alcoholic fatty liver disease, and this association may contribute to the rising incidence of HCC witnessed in many industrialized countries. It is also problematic that HCC may complicate non-cirrhotic, non-alcoholic fatty liver disease with mild or absent fibrosis, greatly expanding the population potentially at higher risk.[5] Because HCC has a poor prognosis due to its aggressive nature, surgical resection and radiofrequency ablation (RFA) are effective only in early stage of HCC.[4,6] Recurrence occurs almost in 70% of patients with HCC of the first occurrence within 5 years.[7] Regarding the treatment of HCC in United

What's new?

The identification of biomolecules associated with hepatocellular carcinoma (HCC) could greatly improve screening for early disease detection. Ubiquitous mitochondrial creatine kinase (uMtCK) could be a promising marker in this context, though its relevance in HCC is unclear, as it may be associated with mitochondrial stability rather than carcinogenesis. Here, in transgenic mice susceptible to the loss of liver mitochondrial integrity, uMtCK was found to be elevated in HCC tissue but not in non-tumorous liver tissue. Increased uMtCK was further linked to reduced expression of ASB9 and elevated risk for HCC-related death.

States veterans, approximately 40% of patients were reportedly diagnosed during hospitalization. Most patients were not seen by a surgeon or oncologist for treatment evaluation and only 34% received treatment.[8] Although there was no effective chemotherapy for advanced HCC for a long time, a novel anti-cancer therapy such as anti-angiogenesis pathway therapy has just recently been developed to prolong survival in patients with the advanced disease.[9,10] However, its effect is rather limited, just extending median survival from 7.9 months to 10.7 months in patients with advanced HCC.[10] Thus, the effective way for early detection of HCC is urgently needed. To this end, the recommended screening strategy for patients with cirrhosis includes the determination of serum alpha-fetoprotein (AFP) levels and an abdominal ultrasound every 6 months to detect HCC at an earlier stage. AFP, however, is a marker characterized by poor sensitivity and specificity.[11] Although other potential markers such as des-gamma-carboxy prothrombin (DCP) and squamous cell carcinoma antigen-immunoglobulin M complex have been proposed to use for diagnosis of HCC, none of them is optimal; however, when used together, their sensitivity in detecting HCC is increased.[11–14] For cholangiocarcinoma, which is a relatively rare type of primary liver cancer that originates in the bile duct epithelium, carbohydrate antigen 19-9, carcinogenic embryonic antigen and cancer antigen 125 have shown sufficient sensitivity and specificity to detect and monitor it. In particular, the combination of these markers seems to increase their efficiency in diagnosing of cholangiocarcinoma.[15]

In this context, we have recently reported that serum mitochondrial creatine kinase (MtCK) activity is increased in patients with HCC, even in those with early stage, suggesting that MtCK may be useful to detect early stage of HCC.[16] Among two tissue-specific isozymes of MtCK, that is, ubiquitous MtCK (uMtCK) and sarcomeric MtCK, we have found that the increase in serum MtCK activity in HCC patients was mostly due to that in serum uMtCK activity but not in serum sarcomeric MtCK activity.[16] Then, we have further observed the higher expression of uMtCK mRNA in HCC cell lines than in normal human liver tissues.[16] Of note, the increased uMtCK expression occurred not only upon malignant changes in the liver, but also in several other malignant tumors such as gastric cancer, breast cancer and lung cancer, where the high expression of uMtCK suggests a poor prognosis.[17–19] In contrast, uMtCK was down-regulated in oral squamous cell carcinoma,[20] and sarcomeric MtCK was also down-regulated during sarcoma development in leg muscle in mice.[21] Therefore, we aimed to elucidate the mechanism(s) and the significance of high uMtCK expression in HCC in this study.

We first examined whether loss of mitochondrial integrity might be involved in high uMtCK expression in HCC, using hepatitis C virus (HCV) core gene transgenic mice. HCV core protein has been first demonstrated to play a pivotal role in HCC development within these transgenic mice, which are known to lose mitochondrial integrity and subsequently develop HCC without apparent inflammation and fibrosis in the liver.[22,23] As a regulatory factor for uMtCK expression, we have focused on the ankyrin repeat and suppressor of cytokine signaling (SOCS) box protein (ASB) family, which reportedly plays an important role in biological processes and regulations of cell proliferation and differentiation. The ASBs have two functional domains: a SOCS box and a variable number of N-terminal ankyrin repeats. Although SOCS domain uses the SH2 domain to recruit substrates, the ankyrin repeat regions serve as a specific protein–protein interaction domain to recruit target substrates.[24] One of ASB family protein, ASB9, was found to interact with brain type of creatine kinase, leading to its degradation.[25] Recently, uMtCK was found to be another ASB9 target.[26] Ankyrin repeat domains of ASB9 associates with the substrate binding site of uMtCK and induce its ubiquitination. Thus, we analyzed the potential association between uMtCK and ASB9 in HCC cell lines, HepG2, PLC/PRF/5, HuH7, in which the expression of uMtCK mRNA was shown to be increased compared with normal liver tissues.[16] To clarify the significance of high uMtCK expression in HCC, we used the siRNA approach to silence uMtCK expression and study its effects on HCC cell lines. Finally, we analyzed the clinical significance of high uMtCK expression in HCC patients who were treated with RFA.

Material and Methods

Materials

Human normal liver RNA was purchased from Cell Applications (San Diego, CA), and human whole liver cell pellets from DV Biologics (Costa Mesa, CA). Specific antibodies against uMtCK and ASB9 were obtained from Abcam (Cambridge, UK), an antibody against caspase 3 from Cell Signaling Technology (3G2; Boston, MA), and an antibody against beta-actin from Sigma–Aldrich (MO).

Cells and cell culture

HCC cell lines, HepG2 and PLC/PRF/5 were obtained from RIKEN BioResource Center (Tsukuba, Ibaraki, Japan) and HuH7 from Health Science Research Resources Bank, Japan Health Science Foundation. HepG2 and PLC/PRF/5 were maintained in RPMI-1640 containing 10% of fetal bovine serum, and HuH7, in Dulbecco's Modified Eagle Medium containing 10% of fetal bovine serum.

Transgenic mice

HCV core gene transgenic mice were produced as previously described.[22] Nontransgenic littermates of the transgenic mice were used as controls. All mice were fed a standard pelleted diet and water *ad libitum* under normal laboratory conditions of 12 hr-light/dark cycles, and received humane care. The experimental protocol was approved by Animal Research Committee of the University of Tokyo.

Quantitative real-time PCR

Total RNA of HCC cell lines (HepG2, PLC/PRF/5 and HuH7), human normal liver and livers from non-transgenic and HCV core gene transgenic mice were extracted using TRIZOL reagent (Invitrogen, CA). One microgram of purified total RNA was transcribed using a SuperScript™ First-Strand Synthesis System for RT-PCR (Invitrogen). Quantitative real-time PCR was performed with a LightCycler FastStart DNA Master SYBR Green I kit (Roche Molecular Diagnostics, CA) or TaqMan Universal Master Mix. The primer pairs used were as follows: human ASB9: 5′-CCTGGCATCAGGCTTCTTTC-3′ and 5′-ACCCCTGGCTGATGAGGTTC-3′[27]; human beta-actin: 5′-GGGTCAGAAGGATTCCTATG-3′ and 5′-CCTTAATGTC ACGCACGATTT-3′.[26] Mouse uMtCK primers and probe were obtained from Applied Biosystems, TaqMan Gene Expression Assays (Mm00438221_m1). The samples were incubated for 10 min at 95°C, followed by 40 cycles at 95°C for 10 sec, 60°C for 10 sec and 72°C for 10 sec. The target gene mRNA expression level was relatively quantified to beta-actin using $2^{-\Delta\Delta Ct}$ method (Applied Biosystems, User Bulletin No 2).

ASB9 transfection

Cells, transiently expressing human ASB9 protein, were constructed using mammalian cell expression vector p3FLAG CMV-10 containing the corresponding cDNA which derived from human normal liver RNA. The primers used for cloning were 5′-GCGGATCCGTCATGGATGGCAAACAAGGG-3′ and 5′-GAGCGGCCGCTTAAGATGTAGGAGAAACTGTT T-3′ which were designed based on human ASB9 reference sequence (NM_001031739.2). The ASB9 cDNA was created by PCR and verified by DNA sequencing.

Immunoblot analysis

Cell and tissue extracts were prepared using M-PER Mammalian Protein Extraction Reagent (Thermo Fisher Scientific, IL) plus Halt™ Protease Inhibitor Cocktail (Thermo Fisher Scientific). Immunoblot analysis was performed as previously described,[28] using NuPAGE SDS-PAGE Gel (Invitrogen) and iBlot Dry Blotting System (Invitrogen) with specific antibodies against uMtCK (dilution 1:1,000), ASB9 (dilution 1:500), caspase 3 (dilution 1:1,000) and beta-actin (dilution 1:2,000). Immunoreactive proteins were visualized using a chemiluminescence kit (GE Healthcare, Buckinghamshire, UK), and recorded using a LAS-4000 image analyzer (Fuji Film, Tokyo, Japan). The intensities of immunodetected bands were quantified with NIH Image J software.

uMtCK siRNA transfection

Cells were transfected with the human uMtCK-specific 23/27mer RNA duplex or a universal negative control duplex at 20 nM, respectively, according to the vender instructions (Integrated DNA Technologies, IA). The human uMtCK-specific RNA duplex used was 5′-UGAAGCACACCACGGAUCU-3′ and 3′-ACUUCGUGUGGUGCCUAGA-5′,[29] negative control RNA duplex, 5′-CGUUAAUCGCGUAUAAUACGCGUAT-3′ and 3′-CAGCAAUUAGCGCAUAUUAUGCGCAUA-5′ (Integrated DNA Technologies). The transfection was performed using Lipofectamine Plus™ (Invitrogen) as described.[29]

Cell membrane integrity and proliferation assays

Cell membrane integrity was determined using the In Vitro Toxicology Assay Kit, Lactic Dehydrogenase based (Sigma–Aldrich). HCC cell lines were inoculated in six-well plates at 2.5×10^5 cells/well and cultured for 24 hr before uMtCK siRNA or universal negative control transfection. Dead cells were assessed at 48 hr after transfection.

Cell proliferation in HCC cell lines was measured at 48 hr after transfection with uMtCK siRNA or universal negative control by determination of BrdU incorporation using the Cell Proliferation ELISA, BrdU colorimetric assay (Roche Applied Science, Upper Bavaria, Germany). In the above two assays, absorbance was measured by plate reader (SPECTRA Thermo, TECAN, Männedorf, Switzerland).

Cell migration and invasion assays

Cell migration and invasion assays were performed according to the vender's instruction (BD, NJ). Cells transfected with uMtCK siRNA or universal negative control were cultured for 24 hr, then 2×10^4 cells were plated into the upper chamber of 24-well plates with 8 μm of pore size in serum-starved condition to examine cell migration and polycarbonate transwell filter chamber coated with Matrigel (BD BioCoat Matrigel Invasion Chamber) to check cell invasion. In both assays, 750 μL medium supplemented with 10% serum was added into the lower chambers. Cells were incubated at 37°C for 22 hr, and the inside chambers were removed with cotton swabs and cells that had transferred to the lower membrane surface were fixed and stained with Diff-Quik stain. Cell counts (four random 100× fields per well) are expressed as the mean number of cells per field of view.

Patients and measurement of MtCK activity

Consecutive 147 HCC patients with cirrhosis caused by hepatitis B virus or HCV, who were admitted into the Department of Gastroenterology, the University of Tokyo Hospital, Tokyo, Japan, between January and April 2010, were previously enrolled to analyze serum MtCK activity.[16] Diagnosis of cirrhosis was based on the presence of clinical and laboratory features indicating portal hypertension, and diagnosis of HCC was made by dynamic CT or MRI.[30,31] Prior to the treatment of HCC, serum MtCK activity was measured[16] with an immuno-inhibition method using the two types of anti-MtCK monoclonal antibodies.[32] Among these patients, 105 patients, who had been successfully treated by RFA without residual HCC after the treatment, were enrolled in the current prognosis analysis. The detailed procedure of RFA has been meticulously described elsewhere.[33] Overall survival of these 105 patients was analyzed from the time of measurement of serum MtCK activity to death related to HCC, excluding the death not associated with HCC expansion or liver insufficiency, such as cardiovascular events or other organ malignancy, or to March 2013.

This study was performed in accordance with the ethical guidelines of the 1975 Declaration of Helsinki and was approved by the Institutional Research Ethics Committees of the authors' institutions. A written informed consent was obtained for the use of the samples in this study.

Statistical analysis

The results of *in vitro* experiments are expressed as the means and standard error of the mean. Student's *t* test (two tailed) was used for comparison unless indicated otherwise. The results were considered significant when *p*-values were 0.05. In the analysis of risk factors for HCC-related death, we tested the following variables obtained at the time of entry on the univariate and multivariate Cox proportional hazard regression analysis: age, sex, hepatitis B infection, serum MtCK activity, serum albumin concentration, aspartate aminotransferase (AST) levels, alanine aminotransferase (ALT) levels, gamma-glutamyltransferase (GGT) levels, total bilirubin concentration, AFP concentration, DCP concentration, platelet count, prothrombin activity and liver stiffness values. Survival and recurrence curves were created using Kaplan–Meier method and compared *via* log-rank test. Data processing and analysis were performed using S-PLUS 2000 (MathSoft, Seattle, WA) and SAS Software version 9.1 (SAS Institute, Cary, NC).

Results

Loss of mitochondrial integrity may not contribute to high expression of uMtCK in HCC

Mutations of mitochondrial DNA have been reported to be involved in hepatocarcinogenesis in humans.[34,35] Furthermore, in a mouse model for hepatocarcinogenesis, oxidative stress was shown to lead to loss of mitochondrial integrity in the liver and ultimately hepatocarcinogenesis.[23] Thus, we wondered whether loss of mitochondrial integrity in the liver might be associated with increased expression of uMtCK in HCC. To examine this idea, we used a transgenic mouse model of HCC in HCV infection (transgenic line S-N/863), with which the direct association between HCV and HCC was first described.[22] In these HCV core gene transgenic mice, loss of mitochondrial integrity has been reported to be observed as early as 2 months of age and increased in an age-dependent manner,[23] and ultimately HCC develops at 19 months of age without apparent inflammation or fibrosis in the liver.[22]

We examined uMtCK mRNA levels in the liver of these HCV core protein transgenic mice at 6 months and 19 months of age. These mice at 6 months of age reportedly develop hepatic steatosis[22] as well as loss of mitochondrial integrity.[23] In these mice at 19 months of age, tumor tissues of HCC and non-tumorous tissues of the liver were analyzed. Non-transgenic mice at 6 months of age were used as control. uMtCK mRNA levels were increased in tumor tissues of HCC in HCV core gene transgenic mice at 19 months of age by 7.7-fold compared to the liver tissues of control mice ($p = 0.02$; Fig. 1*a*). In these HCV core transgenic mice at 19 months of age, uMtCK protein expression was detected in HCC tissues but not in non-tumorous tissues by immunoblot analysis (Fig. 1*b*). These results suggest that hepatocarcinogenesis *per se* but not loss of mitochondrial integrity may contribute to the increase in uMtCK levels in HCC.

Transient expression of ASB9 negatively regulates uMtCK protein levels in HCC cells

It has been reported that ASB protein family is importantly involved in ubiquitination-mediated proteolysis pathway and each member of this large protein family has a different target to be degraded. In ASB protein family, we paid attention to ASB9, which reportedly plays a crucial role in the regulation of the brain type of creatine kinase and uMtCK. HCC cell lines, HepG2, PLC/PRF/5 and HuH7, were selected for *in vitro* experiments, because they had been reported to express high levels of uMtCK mRNA compared to human normal liver tissue.[16] To study whether ASB9 could regulate uMtCK protein levels in these HCC cells, we first measured ASB9 mRNA expression in those cells. Figure 2*a* demonstrates the low ASB9 mRNA expression in HCC cell lines, contrasting with high uMtCK mRNA expression levels in those cells.[16] In line with our mRNA expression data, ASB9 protein levels were almost undetectable in HepG2, PLC/PRF/5 and HuH7 cells comparing to normal whole liver cell pellets (Fig. 2*b*). Further, we investigated the effect of transient overexpression of ASB9 on uMtCK protein levels in HepG2, PLC/PRF/5 and HuH7 cells. Cells were transiently transfected with mammalian cell expression vector p3FLAG-CMV10 containing human ASB9 DNA and harvested at 36 hr after transfection to analyze protein levels. Down-regulation of uMtCK protein levels by transient

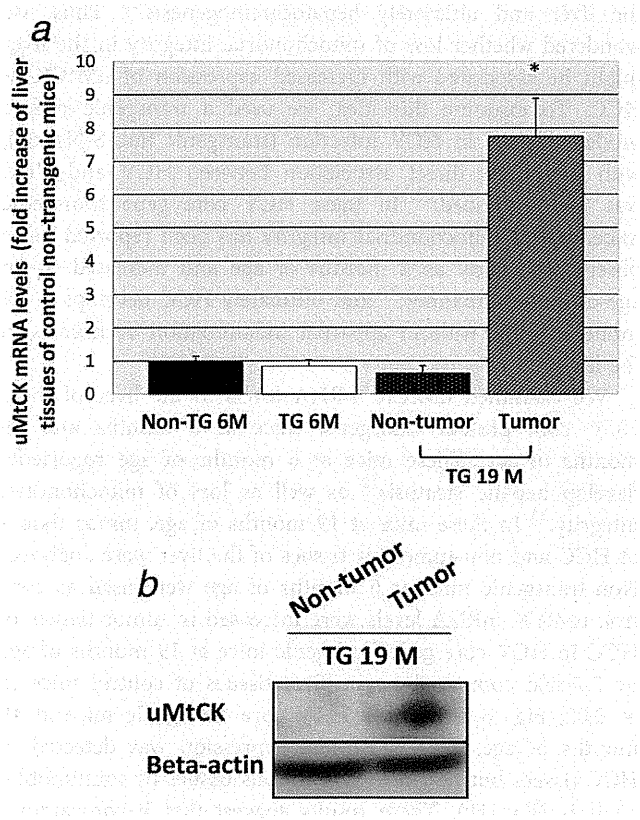

Figure 1. uMtCK mRNA and protein levels in liver tissues of the control non-transgenic, HCV core gene transgenic mice. (*a*) uMtCK mRNA levels were examined by real-time PCR in liver tissues of the control non-transgenic mice (Non-TG) at 6 months of age ($n = 4$), and HCV core gene transgenic mice (TG) at 6 ($n = 4$) and 19 months of age ($n = 4$). For HCV core gene transgenic mice at 19 months of age, HCC tissues and non-tumorous tissues were separately evaluated. Results represent a fold increase level of liver tissues of control non-transgenic mice. An asterisk indicates a significant difference ($p = 0.02$) from liver tissues of non-transgenic mice. (*b*) uMtCK protein levels were analyzed by immunoblotting in HCC tissues and non-tumorous tissues in the livers of HCV core gene transgenic mice at 19 months of age.

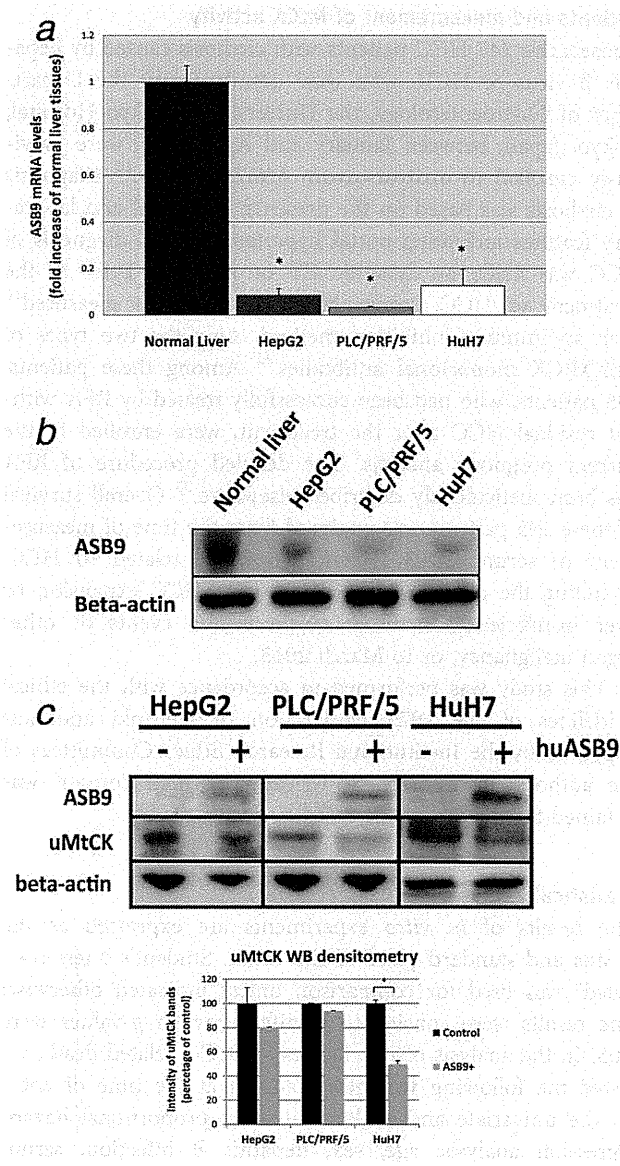

Figure 2. ASB9 expression and the effect of ASB9 transfection on uMtCK protein levels in HCC cells. ASB9 mRNA (*a*) and protein (*b*) levels in HepG2, PLC/PRF/5 and HuH7 cells were examined by real-time PCR and immunoblot analysis, respectively. As a positive control for ASB9 mRNA and protein expressions, human normal liver RNA and human whole liver cell pellets were used. An asterisk indicates a significant difference from normal liver tissue; $p = 0.006$ for HepG2, $p = 0.005$ for PLC/PRF/5 and $p = 0.01$ for HuH7. Increased expression of ASB9 by transfection caused reduced protein levels of uMtCK in HepG2, PLC/PRF/5 and HuH7 cells (*c*). An asterisk indicates a significant difference ($p = 0.007$) from control without ASB9 transfection.

overexpression of ASB9 was observed significantly in HuH7 cells ($p = 0.007$), and a trend of decreased uMtCK protein levels was found in HepG2 and PLC/PRF/5 cells, although not statistically significant (Fig. 2*c*). These results suggest a functional interaction of ASB9 with uMtCK may lead to degradation of uMtCK protein in HCC cell lines, as previously described.[26]

Reduction in uMtCK expression led to increased cell death, and reduced proliferation, migration and invasion of HCC cells

To inhibit high uMtCK expression in HepG2, PLC/PRF/5 and HuH7 cells,[16] isoform-specific siRNA was chosen as described[29] and successfully silenced target protein expression; the results from immunoblot analysis of untransfected and transfected cell lysates with universal negative control and uMtCK siRNA are shown in Figure 3*a*. As expected, in all HCC cell lines transfected with uMtCK siRNA, the expression levels of uMtCK were clearly reduced at 36 hr after transfection (Fig. 3*a*).

Then, the effects of a reduction in uMtCK expression on cell membrane integrity and proliferation were determined in HepG2, PLC/PRF/5 and HuH7 cells. In the first step, we have checked cell membrane integrity by measuring lactate

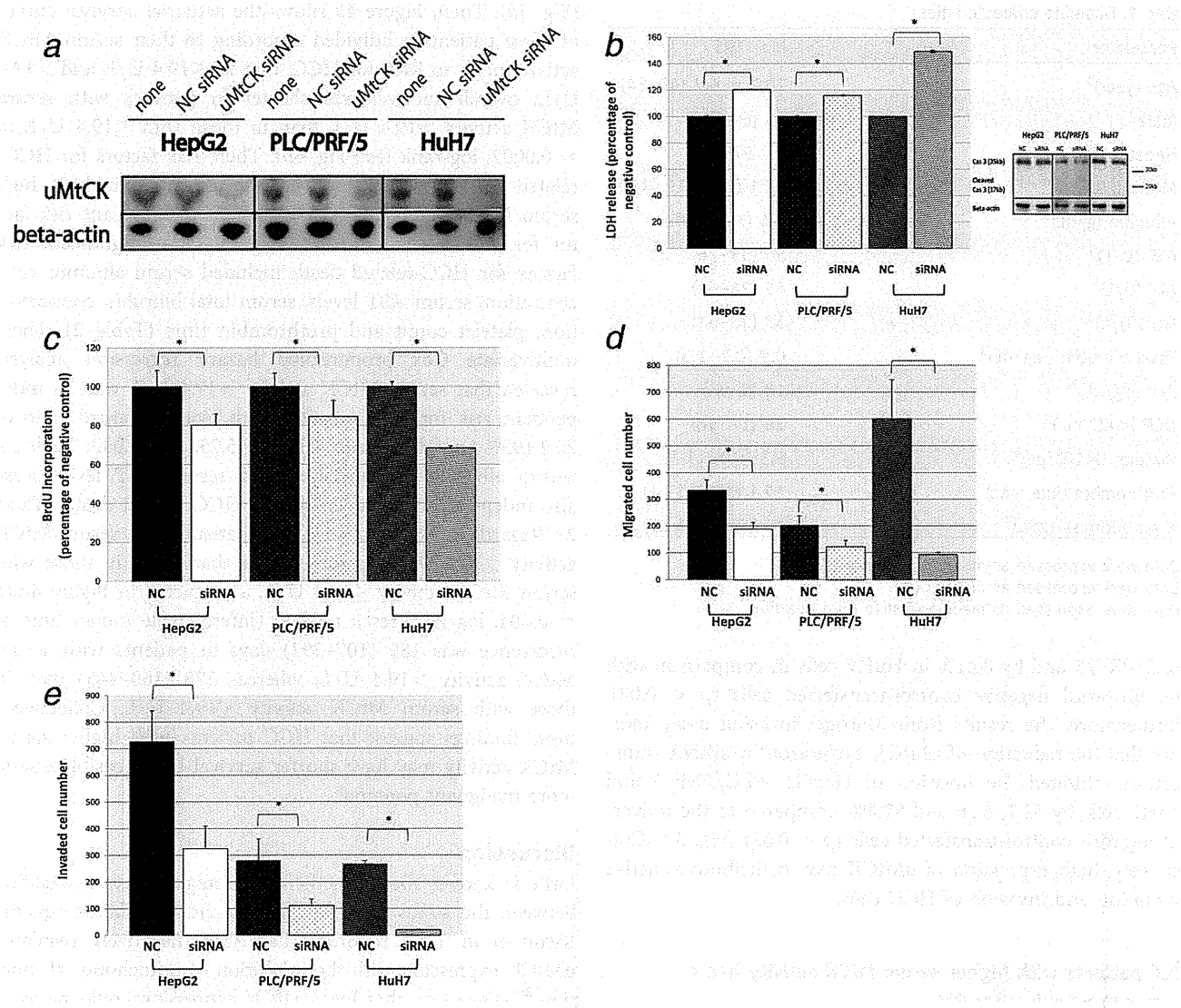

Figure 3. Increase in cell death and reduction in proliferation, migration and invasion by reduced uMtCK expression with siRNA in HCC cell lines. Human HCC cell lines, HepG2, PLC/PRF/5 and HuH7 cells, were transfected with 20 nM uMtCK siRNA or universal negative control, and uMtCK levels were examined by immunoblot analysis. None, no transfection; NC, negative control (*a*). Cell death (*b*), proliferation (*c*), migration (*d*) and invasion (*e*) were assessed in these HCC cell lines treated with or without uMtCK siRNA. An asterisk indicates a significant difference; $p < 0.001$ for cell death and proliferation, $p < 0.02$ for cell migration and invasion from NC.

dehydrogenase released into the culture medium in universal negative control- and uMtCK siRNA-transfected cells (Fig. 3*b*). In all three cells, transfection with uMtCK siRNA led to an increase in the rate of cell lysis by 20.3% in HepG2, by 15.9% in PLC/PRF/5 and by 49.2% in HuH7, compared to respective control cells transfected with universal negative control ($p < 0.001$). However, caspase 3 activity was not altered in uMtCK siRNA-transfected cells compared to universal negative control-transfected cells (Fig. 3*b*), suggesting that lactate dehydrogenase release may be explained by some non-specific cell lysis but not by programmed cell death.

Next, to examine a potential association of the reduction in uMtCK expression with cell proliferation rate, BrdU incorporation assay was performed (Fig. 3*c*). A reduction in cell proliferation was detected in all three HCC cell lines by 19.8% in HepG2, by 15.5% in PLC/PRF/5 and by 31.7% in HuH7, compared to respective control cells transfected with universal negative control ($p < 0.001$). These results suggest that high expression of uMtCK may play a role in sustaining active proliferation of HCC cells.

The ability of a cancer cell to undergo migration and invasion allows the cell to change position within the tissues. To spread within the tissues, tumor cells use migration and invasion mechanisms. Thus, we investigated the effects of uMtCK inhibition on HCC cell migration and invasion by conducting assays for Matrigel-coated chamber migration and invasion. As shown in Figure 3*d*, silencing of uMtCK decreased migration rate by 44.1% in HepG2, by 40.0% in

Table 1. Baseline characteristics

Parameter	$N = 105$
Age (year)[1]	70.7 ± 6.7 (49–84)
Male[2]	63 (60.0)
Hepatitis B/C	8 / 97
MtCK (U/L)[3]	9.71 (5.99–19.44)
Albumin (g/dL)[3]	3.4 (3.1–3.9)
AST (U/L)[3]	55 (35–76)
ALT (U/L)[3]	45 (26–60)
GGT (U/L)[3]	37 (28–62)
Total bilirubin (mg/dL)[3]	0.9 (0.7–1.3)
AFP (ng/dL)[3]	18 (8–66)
DCP (mAU/mL)[3]	26 (17–58)
Platelet ($\times 10^4/\mu L$)[3]	9.3 (6.3–11.7)
Prothrombin time (sec)[3]	12.1 (11.5–13.1)
Liver stiffness (kPa)[3]	26.3 (18.8–42.2)

[1]Data were expressed as mean ± SD (range).
[2]Data were expressed as number (%).
[3]Data were expressed as median (first to third quartile).

PLC/PRF/5 and by 84.1% in HuH7 cells in comparison with the universal negative control-transfected cells ($p < 0.02$). Furthermore, the results from Matrigel invasion assay indicate that the reduction of uMtCK expression by siRNA transfection inhibited the invasion of HepG2, PLC/PRF/5 and HuH7 cells by 51.7, 62.6 and 92.4%, compared to the universal negative control-transfected cells ($p < 0.02$) (Fig. 3*e*). Collectively, high expression of uMtCK may contribute to active migration and invasion of HCC cells.

HCC patients with higher serum MtCK activity had a poorer prognosis after RFA

Because above *in vitro* results using HCC cell lines suggest that HCC cells with higher expression of uMtCK may have more malignant potential, we next examined a potential association between serum MtCK activity and prognosis in patients with HCC. As described earlier, among two tissue-specific isozymes of MtCK, that is, uMtCK and sarcomeric MtCK, the increase in serum MtCK activity in HCC patients was mostly due to that in serum uMtCK activity but not in serum sarcomeric MtCK activity.[16] To this end, a prognosis of HCC patients, who had been previously enrolled to examine their serum MtCK activity and successfully treated by RFA without residual HCC after the treatment, was analyzed. Characteristics of these 105 HCC patients are shown in Table 1. During the mean follow-up period of 848 days, HCC-related death was observed in 17 patients. First, to evaluate the potential ability of MtCK values to predict survivals or death, a receiver operating characteristic (ROC) curve was generated. The ROC curve showed that a MtCK cutoff of 19.4 U/L had a sensitivity of 76.9% and a specificity of 83.8% for discriminating survivors and deceased patients (Fig. 4*a*). Then, Figure 4*b* shows the actuarial survival curves of these patients subdivided according to their serum MtCK activity prior to RFA for HCC, that is, ≤19.4 U/L and >19.4 U/L; overall survival was shorter in patients with serum MtCK activity >19.4 U/L than in those with ≤19.4 U/L ($p = 0.0002$; log-rank test; Fig. 4*b*). Then, risk factors for HCC-related death were analyzed. On the univariate analysis, high serum MtCK activity (>19.4 U/L) was a significant risk factor for HCC-related death (Table 2). Other significant risk factors for HCC-related death included serum albumin concentration, serum AST levels, serum total bilirubin concentration, platelet count and prothrombin time (Table 2). Then, multivariate Cox proportional hazard regression analysis revealed that serum MtCK activity >19.4 U/L was an independent risk for HCC-related death, with a hazard ratio of 2.32 (95% confidence interval: 1.03–5.25; $p = 0.042$; Table 2). Serum albumin concentration and serum AST levels were also independently associated with HCC-related death (Table 2). Regarding recurrence, HCC in patients with serum MtCK activity >19.4 U/L recurred earlier than HCC in those with serum MtCK activity ≤19.4 U/L, as depicted in Figure 4*c* ($p = 0.004$; log-rank test); median (interquartile range) time to recurrence was 189 (107–292) days in patients with serum MtCK activity >19.4 U/L, whereas 278 (160–445) days in those with serum MtCK activity ≤19.4 U/L. Collectively, these findings suggest that HCC patients with higher serum MtCK activity may have shorter survival time possibly due to more malignant potential.

Discussion

Little is known about whether there might be an association between the status of mitochondria and uMtCK expression. Kwon *et al.* have reported that ASB9 negatively regulated uMtCK expression with the inhibition of mitochondrial function,[26] suggesting that low uMtCK expression could be associated with loss of mitochondrial integrity. There could be several possibilities regarding the status of mitochondria and uMtCK expression in the liver or HCC; one is that loss of mitochondrial integrity might be associated with reduced uMtCK expression as previously reported.[26] As another possibility, uMtCK expression might be increased as a compensatory mechanism with loss of mitochondrial integrity. In fact, this is exactly the case with sarcomeric MtCK in mitochondrial myopathies.[36] It is also possible that there might be no association in general between loss of mitochondrial integrity and uMtCK expression. In this context, we wondered whether loss of mitochondrial integrity in the liver might be involved in the mechanism of increased uMtCK expression in HCC. To examine this, HCV core gene transgenic mice were used, because these mice develop HCC with loss of mitochondrial integrity in the liver in the absence of inflammation and fibrosis.[22,23] As a result, uMtCK expression was essentially not altered in non-tumorous liver tissues with loss of mitochondrial integrity but clearly enhanced in HCC tissues, suggesting that hepatocarcinogenesis *per se* but not

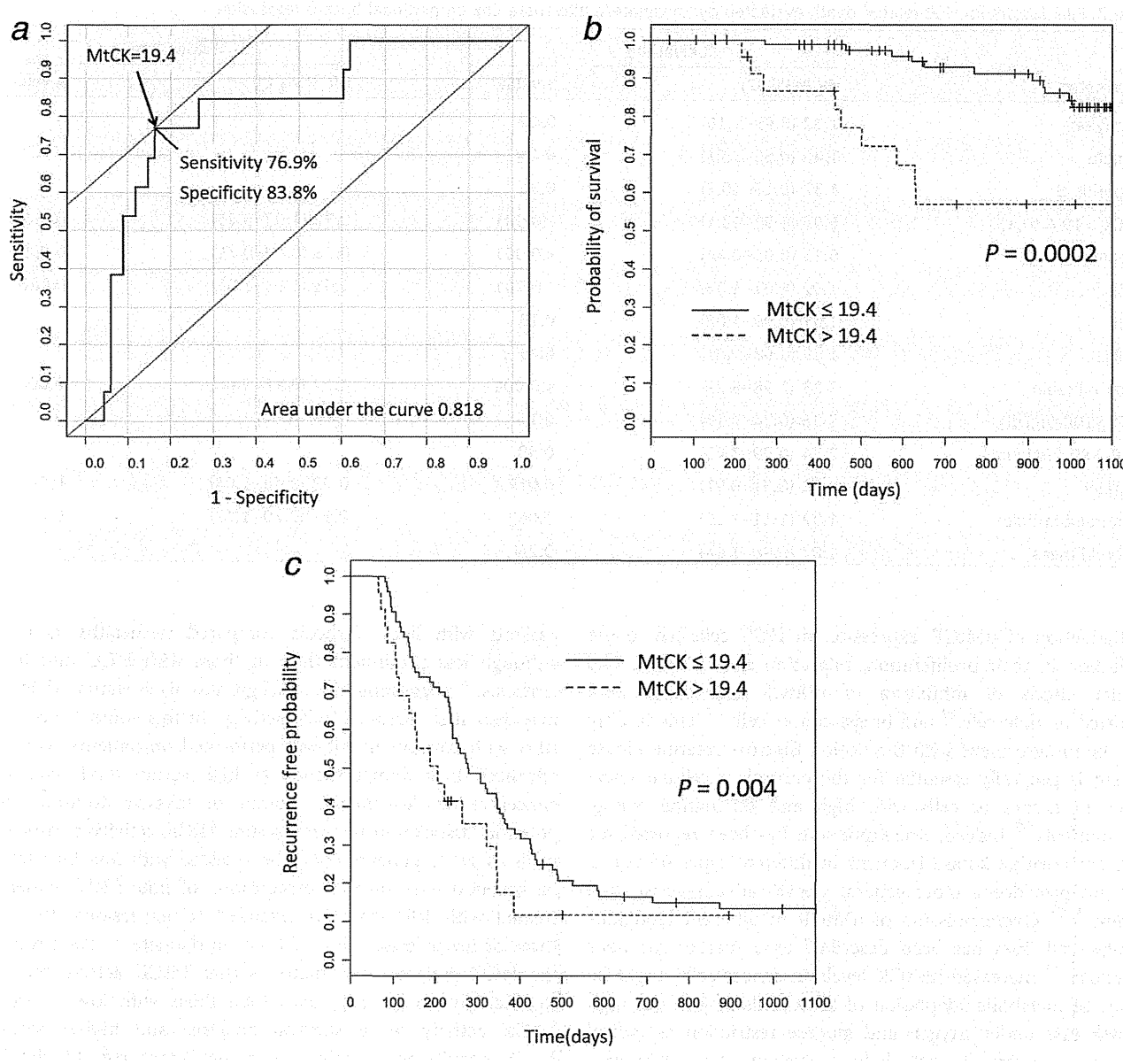

Figure 4. (*a*) ROC curve showing the overall accuracy of serum MtCK activity for discriminating between survivors and deceased patients. The arrow identifies the best cutoff value (*i.e.*, 19.4 U/L) of serum MtCK activity. Kaplan–Meier survival (*b*) and recurrence (*c*) curve of the studied patients subdivided according to their serum MtCK activity prior to RFA for HCC. Solid line, ≤19.4 U/L; dashed line, >19.4 U/L.

loss of mitochondrial integrity may contribute to increased uMtCK expression in HCC.

Regarding the regulatory mechanism(s) of increased uMtCK expression in HCC, we have found that ASB9 interacted with uMtCK to reduce its protein levels in HCC cells, similarly to HEK293 cells as previously described.[26] In normal liver, uMtCK levels are generally at a very low level, while sarcomeric MtCK as a muscle-specific isoform is not expressed at all,[37] whereas ASB9 mRNA expression is reportedly abundant.[26] Thus, ASB9 may play a physiological role to keep uMtCK protein levels low in the liver. Regarding HCC, ASB9 mRNA expression in HCC cells were much lower than that in normal liver tissue in the current study. This finding raises the possibility that low expression of ASB9 may explain, at least in part, high protein levels of uMtCK in HCC. Collectively, we may suggest that the two possible mechanisms of increased uMtCK protein levels in HCC cells should be increased gene expression and decreased protein degradation due to reduced ASB9 expression. It has been reported that colorectal cancer with low ASB9 expression may have a higher malignant potential and a poorer prognosis than that with high ASB9 expression,[27] suggesting a negative association of ASB9 with uMtCK protein levels also in colorectal cancer cells. Nonetheless, a potential role of ASB9 in the regulation of uMtCK expression in HCC *in vivo* should be further elucidated.

Table 2. Risk factors for HCC-related death evaluated by univariate/multivariate Cox proportional hazard regression

	Univariate		Multivariate	
Parameter	HR (95% CI)	*p* value	HR (95% CI)	*p* value
Age (year)	1.02 (0.95–1.10)	0.60		
Female	1.45 (0.56–3.77)	0.44		
Hepatitis B	1.37 (0.18–10.3)	0.76		
MtCK >19.4 (U/L)	5.03 (1.93–13.1)	<0.001	2.32 (1.03–5.25)	0.042
Albumin	0.15 (0.05–0.44)	<0.001	0.26 (0.09–0.71)	0.009
AST	1.02 (1.01–1.03)	<0.001	1.01 (1.00–1.02)	0.028
ALT	1.01 (0.99–1.02)	0.13		
GGT	1.00 (0.98–1.01)	0.45		
Total bilirubin	3.23 (1.98–5.29)	<0.001	1.72 (0.97–3.04)	0.064
AFP >100 (ng/dL)	2.28 (0.84–6.18)	0.11		
DCP >80 (mAU/mL)	2.74 (0.99–7.45)	0.59		
Platelet	0.83 (0.71–0.97)	0.017	0.89 (0.76–1.04)	0.14
Prothrombin time	1.32 (1.11–1.57)	0.002	0.91 (0.70–1.17)	0.45
Liver stiffness	1.02 (0.98–1.04)	0.25		

Reduction of uMtCK expression in HCC cells led to the inhibition in their proliferation, migration and invasion. The similar effects of inhibition of uMtCK expression were reported in Hela cells[29] and breast cancer cells.[17] This finding may be in agreement with the notion that the creatine kinase system is generally essential for the control of cellular energetics in tissues or cells with high and fluctuating energy requirements.[37] Indeed, overexpression has been reported for different creatine kinase isoforms in different types of cancer and has provided a more general growth advantage to solid tumors.[37,38] Overexpression of uMtCK in different Hodgkin-derived cell lines has been described as a marker for poor prognosis.[39] Increased uMtCK levels in cancer cells might be a part of metabolic adaptation of those cells to perform high growth rate under oxygen and glucose restriction as typical for many cancers; it could help to sustain energy turnover, but would be also protective against stress situations such as hypoxia and possibly protect cells from death.[40] Nonetheless, these *in vitro* findings raise the possibility that high expression of uMtCK in HCC may be associated with its active growth and metastasis.

Then, we performed a follow-up study of the HCC patients, with whom we showed the increased serum MtCK activity.[16] Among the entire HCC patients in the previous study, we enrolled the patients who underwent RFA with curative intent to examine the potential association between serum MtCK activity and prognosis in this study. In the previous report, serum MtCK activity was also enhanced in the patients with liver cirrhosis compared to healthy control, although less prominent than in those with HCC and liver cirrhosis,[16] suggesting that background liver status of HCC may also affect serum MtCK activity. In this context, because RFA with curative intent was performed on patients without advanced liver damages such as high serum total bilirubin concentration, low platelet counts or massive ascites,[33] the potential association between serum MtCK activity and prognosis of HCC patients could be assessed with less bias from background liver status. Furthermore, of note, HCC patients treated with RFA had no extended tumor lesions, that is, three or fewer lesions, each 3.0 cm in diameter.[33] As a result, the HCC patients with higher serum MtCK activity had a significantly poorer prognosis than those with lower serum MtCK activity on a survival analysis, and higher serum MtCK activity was retained as a significant risk for HCC-related death on multivariate analysis. Thus, in line with the current *in vitro* findings, it is suggested that HCC with increased uMtCK expression may have highly malignant potential.

In conclusion, high uMtCK expression in HCC may be caused by hepatocarcinogenesis *per se* but not by loss of mitochondrial integrity, and associated with highly malignant potential, where ASB9 could be one of the regulators of uMtCK expression. In the clinical setting, higher serum MtCK activity was associated with a poorer prognosis of HCC, suggesting that HCC with high serum MtCK activity should be thoroughly treated when considered to be curative.

References

1. Umemura T, Ichijo T, Yoshizawa K, et al. Epidemiology of hepatocellular carcinoma in Japan. *J Gastroenterol* 2009;44 Suppl 19:102–7.
2. Ferlay J, Shin HR, Bray F, et al. Estimates of worldwide burden of cancer in 2008: GLOBOCAN 2008. *Int J Cancer* 2010;127:2893–917.
3. Bosch FX, Ribes J, Cleries R, et al. Epidemiology of hepatocellular carcinoma. *Clin Liver Dis* 2005; 9:191–211.

4. El-Serag HB, Rudolph KL. Hepatocellular carcinoma: epidemiology and molecular carcinogenesis. *Gastroenterology* 2007;132:2557–76.
5. Baffy G, Brunt EM, Caldwell SH. Hepatocellular carcinoma in non-alcoholic fatty liver disease: an emerging menace. *J Hepatol* 2012;56:1384–91.
6. El-Serag HB, Mason AC. Rising incidence of hepatocellular carcinoma in the United States. *N Engl J Med* 1999;340:745–50.
7. Nakakura EK, Choti MA. Management of hepatocellular carcinoma. *Oncology (Williston Park)* 2000;14:1085–98; discussion 98–102.
8. Davila JA, Kramer JR, Duan Z, et al. Referral and receipt of treatment for hepatocellular carcinoma in United States veterans: effect of patient and nonpatient factors. *Hepatology* 2013;57:1858–68.
9. El-Serag HB, Marrero JA, Rudolph L, et al. Diagnosis and treatment of hepatocellular carcinoma. *Gastroenterology* 2008;134:1752–63.
10. Llovet JM, Ricci S, Mazzaferro V, et al. Sorafenib in advanced hepatocellular carcinoma. *N Engl J Med* 2008;359:378–90.
11. Bertino G, Ardiri A, Malaguarnera M, et al. Hepatocellualar carcinoma serum markers. *Semin Oncol* 2012;39:410–33.
12. Bertino G, Ardiri AM, Boemi PM, et al. A study about mechanisms of des-gamma-carboxy prothrombin's production in hepatocellular carcinoma. *Panminerva Med* 2008;50:221–6.
13. Bertino G, Neri S, Bruno CM, et al. Diagnostic and prognostic value of alpha-fetoprotein, des-gamma-carboxy prothrombin and squamous cell carcinoma antigen immunoglobulin M complexes in hepatocellular carcinoma. *Minerva Med* 2011; 102:363–71.
14. Bertino G, Ardiri AM, Calvagno GS, et al. Prognostic and diagnostic value of des-gamma-carboxy prothrombin in liver cancer. *Drug News Perspect* 2010;23:498–508.
15. Malaguarnera G, Paladina I, Giordano M, et al. Serum markers of intrahepatic cholangiocarcinoma. *Dis Markers* 2013;34:219–28.
16. Soroida Y, Ohkawa R, Nakagawa H, et al. Increased activity of serum mitochondrial isoenzyme of creatine kinase in hepatocellular carcinoma patients predominantly with recurrence. *J Hepatol* 2012;57:330–6.
17. Qian XL, Li YQ, Gu F, et al. Overexpression of ubiquitous mitochondrial creatine kinase (uMtCK) accelerates tumor growth by inhibiting apoptosis of breast cancer cells and is associated with a poor prognosis in breast cancer patients. *Biochem Biophys Res Commun* 2012;427:60–6.
18. Kanemitsu F, Kawanishi I, Mizushima J, et al. Mitochondrial creatine kinase as a tumor-associated marker. *Clin Chim Acta* 1984;138:175–83.
19. Pratt R, Vallis LM, Lim CW, et al. Mitochondrial creatine kinase in cancer patients. *Pathology* 1987;19:162–5.
20. Onda T, Uzawa K, Endo Y, et al. Ubiquitous mitochondrial creatine kinase downregulated in oral squamous cell carcinoma. *Br J Cancer* 2006; 94:698–709.
21. Patra S, Bera S, SinhaRoy S, et al. Progressive decrease of phosphocreatine, creatine and creatine kinase in skeletal muscle upon transformation to sarcoma. *FEBS J* 2008;275:3236–47.
22. Moriya K, Fujie H, Shintani Y, et al. The core protein of hepatitis C virus induces hepatocellular carcinoma in transgenic mice. *Nat Med* 1998;4: 1065–7.
23. Moriya K, Nakagawa K, Santa T, et al. Oxidative stress in the absence of inflammation in a mouse model for hepatitis C virus-associated hepatocarcinogenesis. *Cancer Res* 2001;61:4365–70.
24. Kile BT, Schulman BA, Alexander WS, et al. The SOCS box: a tale of destruction and degradation. *Trends Biochem Sci* 2002;27:235–41.
25. Debrincat MA, Zhang JG, Willson TA, et al. Ankyrin repeat and suppressors of cytokine signaling box protein asb-9 targets creatine kinase B for degradation. *J Biol Chem* 2007;282: 4728–37.
26. Kwon S, Kim D, Rhee JW, et al. ASB9 interacts with ubiquitous mitochondrial creatine kinase and inhibits mitochondrial function. *BMC Biol* 2010;8:23.
27. Tokuoka M, Miyoshi N, Hitora T, et al. Clinical significance of ASB9 in human colorectal cancer. *Int J Oncol* 2010;37:1105–11.
28. Ikeda H, Nagashima K, Yanase M, et al. Involvement of Rho/Rho kinase pathway in regulation of apoptosis in rat hepatic stellate cells. *Am J Physiol Gastrointest Liver Physiol* 2003;285:G880–6.
29. Lenz H, Schmidt M, Welge V, et al. Inhibition of cytosolic and mitochondrial creatine kinase by siRNA in HaCaT- and HeLaS3-cells affects cell viability and mitochondrial morphology. *Mol Cell Biochem* 2007;306:153–62.
30. Makuuchi M, Kokudo N, Arii S, et al. Development of evidence-based clinical guidelines for the diagnosis and treatment of hepatocellular carcinoma in Japan. *Hepatol Res* 2008;38:37–51.
31. Torzilli G, Minagawa M, Takayama T, et al. Accurate preoperative evaluation of liver mass lesions without fine-needle biopsy. *Hepatology* 1999;30:889–93.
32. Hoshino T, Sakai Y, Yamashita K, et al. Development and performance of an enzyme immunoassay to detect creatine kinase isoenzyme MB activity using anti-mitochondrial creatine kinase monoclonal antibodies. *Scand J Clin Lab Invest* 2009;69:687–95.
33. Omata M, Tateishi R, Yoshida H, et al. Treatment of hepatocellular carcinoma by percutaneous tumor ablation methods: ethanol injection therapy and radiofrequency ablation. *Gastroenterology* 2004;127:S159–66.
34. Nishikawa M, Nishiguchi S, Shiomi S, et al. Somatic mutation of mitochondrial DNA in cancerous and noncancerous liver tissue in individuals with hepatocellular carcinoma. *Cancer Res* 2001;61:1843–5.
35. Tamori A, Nishiguchi S, Nishikawa M, et al. Correlation between clinical characteristics and mitochondrial D-loop DNA mutations in hepatocellular carcinoma. *J Gastroenterol* 2004;39: 1063–8.
36. Stadhouders AM, Jap PH, Winkler HP, et al. Mitochondrial creatine kinase: a major constituent of pathological inclusions seen in mitochondrial myopathies. *Proc Natl Acad Sci USA* 1994; 91:5089–93.
37. Schlattner U, Tokarska-Schlattner M, Wallimann T. Mitochondrial creatine kinase in human health and disease. *Biochim Biophys Acta* 2006;1762: 164–80.
38. Wyss M, Kaddurah-Daouk R. Creatine and creatinine metabolism. *Physiol Rev* 2000;80: 1107–213.
39. Kornacker M, Schlattner U, Wallimann T, et al. Hodgkin disease-derived cell lines expressing ubiquitous mitochondrial creatine kinase show growth inhibition by cyclocreatine treatment independent of apoptosis. *Int J Cancer* 2001;94: 513–9.
40. Dang CV, Semenza GL. Oncogenic alterations of metabolism. *Trends Biochem Sci* 1999;24:68–72.

OPEN

Gene Therapy (2015), 1–9

www.nature.com/gt

ORIGINAL ARTICLE

Preferable sites and orientations of transgene inserted in the adenovirus vector genome: The E3 site may be unfavorable for transgene position

M Suzuki, S Kondo, Z Pei[1], A Maekawa, I Saito and Y Kanegae

The adenovirus vector (AdV) can carry two transgenes in its genome, the therapeutic gene and a reporter gene, for example. The E3 insertion site has often been used for the expression of the second transgene. A transgene can be inserted at six different sites/orientations: E1, E3 and E4 sites, and right and left orientations. However, the best combination of the insertion sites and orientations as for the titers and the expression levels has not sufficiently been studied. We attempted to construct 18 AdVs producing GFP or LacZ gene driven by the EF1α promoter and Cre gene driven by the α-fetoprotein promoter. The AdV containing GFP gene at E3 in the rightward orientation (GFP-E3R) was not available. The LacZ-E3R AdV showed 20-fold lower titer and 50-fold lower level of fiber mRNA than the control E1L AdV. Notably, we found four aberrantly spliced mRNAs in the LacZ-E3L/R AdVs, probably explaining their very low titers. Although the transgene expression levels in the E4R AdVs were about threefold lower than those in the E1L AdVs, their titers are comparable with that of E1L AdVs. We concluded that E1L and E4R sites/orientations are preferable for expressing the main target gene and a second gene, respectively.

Gene Therapy advance online publication, 15 January 2015; doi:10.1038/gt.2014.124

INTRODUCTION

First-generation (E1 deleted) adenovirus vectors (FG AdVs), which lack the E1 and E3 regions, are popularly used in basic studies to elucidate gene functions, and have been employed for gene therapy.[1–4] Because the DNA fragments of up to about 7 kilobases (kb) in total can be inserted into the AdV genome, the AdVs are frequently used to produce two proteins simultaneously from two independent transgenes expressing both the target gene and the reporter gene, for example. In the studies using the cultured cells and in the animal experiments, the GFP and luciferase are used as the reporters. Recently, positron emission tomography has clinically been used in patients for diagnoses and in experimental animal models. Therefore, the AdVs containing both the therapeutic gene and the positron emission tomography reporter gene would be valuable in the gene therapy fields, because the therapeutic effects, the vector duration and distribution can simultaneously be monitored.[5–8] Probably one would wish for high-titer AdVs with the highest expression for the therapeutic gene and with the second highest for the reporter gene not causing any trouble, if the insertion sites and orientations in the AdV genome can be chosen. However, the titers and the expression levels of the AdVs may considerably be influenced by the sites and orientations of the transgenes. Such information may be very valuable for construction of the best vector, especially in the vector containing both the therapeutic gene and the reporter gene.

The simultaneous expression of two genes could be achieved by inserting the two genes into the E1 site under the control of a single prompter using the internal ribosomal entry sites or using porcine teschovirus-1 2A.[9,10] In the former approach, the expression of the second gene might be influenced by the sequences between internal ribosomal entry sites and its initiation codon, and in the latter, the manipulation is necessary to remove the stop codon of the first gene and to adjust the frames of the two genes. When two genes driven by the independent promoters are inserted into the E1 site, they might interfere with each other. However, when two independent expression units are inserted in different sites in the AdV genome, no interference occurs. Moreover, the advantage of this approach is that the main target gene can easily be changed using the AdV cassette that already contains the reporter gene.

There are three insertion sites and two orientations: a transgene can be inserted into the AdV genome by substitution of the E1 or E3 gene and by simple insertion at a position upstream of the E4 gene. Therefore, there are six different possible sites/orientations for any given transgene. Moreover, not only the potent promoters such as EF1α but also tissue-specific promoters such as α-fetoprotein (AFP) can also be employed. Although the studies examining which sites/orientations are superior to others are practically important, they have been very limited[11,12] and systematic analyses have not been reported so far.

As it is known that the expression level of a transgene varies considerably depending on the site in the cell chromosome of the human genome, the phenomenon is called the 'position effect'.[13,14] Although CG-methylation in the cell chromosome is clearly one reason, it is not observed in the AdV genome. Therefore, it would be of interest to examine whether the 'position effect' might also be observed similarly in the AdV genome for the potent promoter and for the tissue-specific promoter.

Laboratory of Molecular Genetics, The Institute of Medical Science, The University of Tokyo, Minato-ku, Tokyo, Japan. Correspondence: Dr Y Kanegae, Laboratory of Molecular Genetics, The Institute of Medical Science, The University of Tokyo, 4-6-1 Shirokanedai, Minato-ku, 108-8639, Tokyo, Japan.
E-mail: kanegae@ims.u-tokyo.ac.jp
[1]Current address: CDM (Contract Development & Manufacturing) center, Takara Bio Inc., 3-4-1 Seta, Otsu, Shiga, Japan.
Received 15 August 2014; revised 5 November 2014; accepted 20 November 2014

FG AdVs retain almost all viral genes. They are normally not expressed in the target cells, because E1A protein, the essential transactivator for expression of all other viral genes, is not present. However, there is one report of splicing of aberrant mRNAs from the inserted foreign genes to a viral gene.[15] In this case, the aberrant mRNAs are transcribed by strong foreign promoters and produce transgene-viral gene fusion proteins, which elicit strong immune responses. However, it is not known whether the production of the aberrant gene product between the inserted transgene and viral gene is rare or not.

In this study, we examined the AdV titers and expression levels of an identical transgene inserted at the E1, E3 and E4 sites. We used three transgenes, namely, GFP, LacZ and Cre, and two promoters, namely, the potent EF1α promoter and the cancer-specific AFP promoter, and attempted to construct AdVs using all combinations, that is, 18 AdVs, and succeeded in constructing 17 of them. We found that insertion at the E1 and E4 sites yielded mostly high titers, whereas the one at the E3 yielded variable titers. Surprisingly, four aberrantly spliced mRNAs between the transgenes and viral genes were found in the vector obtained by insertion at the E3 site, which was probably the reason for the very low titers. As for the expression levels, clear differences were observed among the vectors obtained with insertion at the E1, E3 and E4 sites despite using the identical transgene, indicating that the position effect was certainly present for the AdV genome and that aberrant splicing may, at least in part, explain this effect. We also propose a strategy to avoid generation of the aberrantly spliced mRNAs.

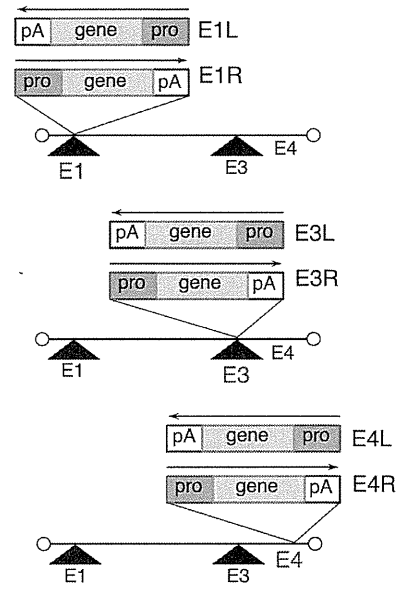

Figure 1. The FG AdV structures of six different site/orientations in all possible combinations. The box containing 'pro,' 'gene' and 'pA' represents the expression unit and the arrows show the orientation of transcription. 'pro,' EF1α and AFP promoter; gene, GFP, LacZ and Cre; pA, rabbit β-globin polyadenylation signal. For example, the vector containing the transgene at the E1 insertion site and in the left orientation is denoted as 'E1L.'

RESULTS

The vector titers were significantly influenced by the insertion sites and orientations of the transgene

We first examined whether the vector titers were influenced by the site/orientations of the transgenes containing a potent EF1α promoter. Towards this end, we attempted to construct six GFP-expressing (EF-GFP) and six LacZ-expressing (EF-LacZ) vectors in all possible combinations, that is, the E1, E3 and E4 insertion sites and the two orientations (Figure 1), and measured the vector titers (Figure 2a) (hereinafter, the vectors will be designated as per the following; the vectors containing the GFP gene and LacZ gene at the E1 insertion site and in the left orientation shall be denoted as G-E1L and Z-E1L vectors, respectively). Among the GFP-expressing vectors, high titers were obtained for G-E1L, G-E3L, G-E4L and G-E4R vectors (Figure 2a, bars 1, 3, 5 and 6), while the titer for the G-E1R vector was lower (bar 2). Notably, the G-E3R vector, that is, vector with the GFP transgene inserted in the E3 site in the rightward orientation, could not be obtained despite three independent attempts (bar 4, denote '×'). Therefore, although exactly the same EF1α-GFP expression unit was inserted in these vectors, the sites and orientations exerted considerable influence on the vector titers and even determined whether the vector was available or not. Similar results were obtained for vectors expressing LacZ: the titers of the Z-E1L, Z-E4L and Z-E4R vectors (bars 7, 11 and 12) were high, and that of the Z-E1R vector was also low (bar 8). However, the results of insertion at the E3 site differed for GFP and LacZ. The titer ratio of Z-E3L was significantly lower than that of G-E3L (compare bars 3 and 9, described later), and the Z-E3R vector was available, although its titer was extremely low (bar 10). Therefore, the GFP gene and LacZ gene themselves influenced the vector titers.

Then, we constructed six vectors containing the AFP promoter and Cre gene (AFP-Cre) and measured their titers (Figure 2b). Although these vectors contained the AFP promoter and Cre gene, this transgene unit served as a nonfunctional DNA, because the AFP promoter, which is hepatocarcinoma-cell-specific, is not active in the 293 cells. The titers of the all six vectors were very similar (Figure 2b). Thus, the site/orientation does not always influence the vector titers, and it appeared that there may be some specific reasons why the titers were low for vectors containing the EF1α promoter expressing the GFP and LacZ genes.

Aberrant chimera mRNAs were produced in the vectors containing the expression unit at the E3 site

The E3 transgene is present within the large intron from the major late promoter (MLP) to the fiber gene (Figure 3a, except the first). We previously reported an aberrant splicing from a cryptic donor site present in the LacZ gene to the viral pIX acceptor site, which produces a LacZ-pIX fusion protein.[15] Therefore, we speculated that similar aberrant splicing might occur for the LacZ gene inserted at the E3 site.

Total RNA was prepared from the 293 cells infected with the E3R vector and reverse-transcribed to detect such aberrantly spliced mRNA spanning from the LacZ cryptic donor site to the possible fiber acceptor site, which is the only acceptor site present downstream of the LacZ donor site. In fact, we identified an aberrant mRNA spliced from this LacZ donor to the fiber acceptor (Figure 3a, second; Figure 3b, 0.7-kb band). The splicing donor site in the LacZ gene was identical to that of the reported LacZ gene inserted at E1 site to the viral pIX acceptor site, and the fiber acceptor site was the same as that normally spliced from the MLP donor site (Supplementary Table S1). This is quite abnormal because, in general, splicing occurs between only specific donor and acceptor sites, suggesting that an inserted transgene could disturb normal splicing.

We also examined whether any other aberrantly spliced mRNA upstream of the transgene was present or not. Surprisingly, we also detected an abnormal mRNA spliced from the donor site of the third exon of the viral MLP to the acceptor site of the second exon of the EF1α promoter (Figure 3a, third; Figure 3b, 1.2-kb band; the junction sequence is shown in Supplementary Table S1). These results mean that the normal splicing from the MLP donor to the fiber acceptor are doubly competed with aberrant splicing

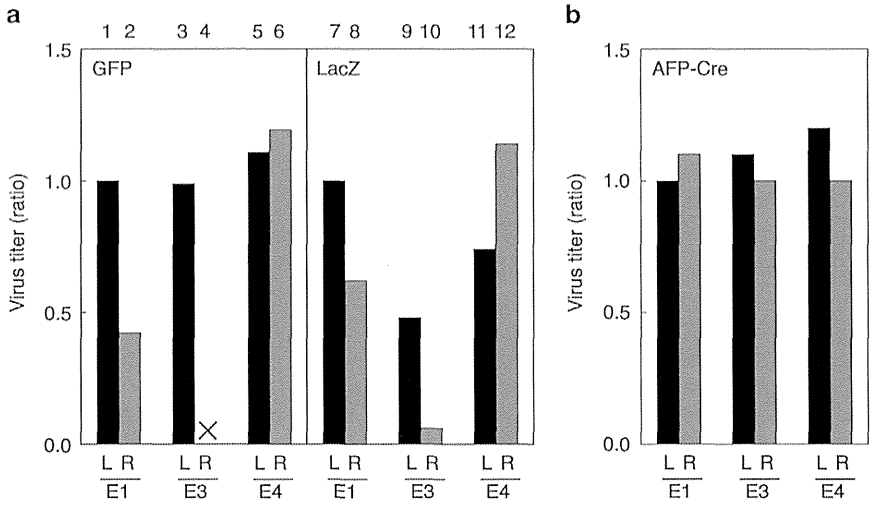

Figure 2. Titers of the virus vectors containing identical expression units. (**a**) Virus titers of the AdVs containing the EF1α promoter. The AdV genomes transduced into the HuH-7 cells were measured 3 days post infection. The virus titers were calculated relative to the copy numbers of the AdVs.[16] The titer of the E1L vector was set as 1; G-E1L, 8.3×10^8 relative virus titer (rVT)/ml, L-E1L, 5.0×10^9 rVT/ml. '×' indicates that G-E3R could not be obtained. (**b**) The titers of the virus vector containing Cre gene driven by the AFP promoter. E1L vector was used as the control. $^*P < 0.05$, $^{**}P < 0.01$.

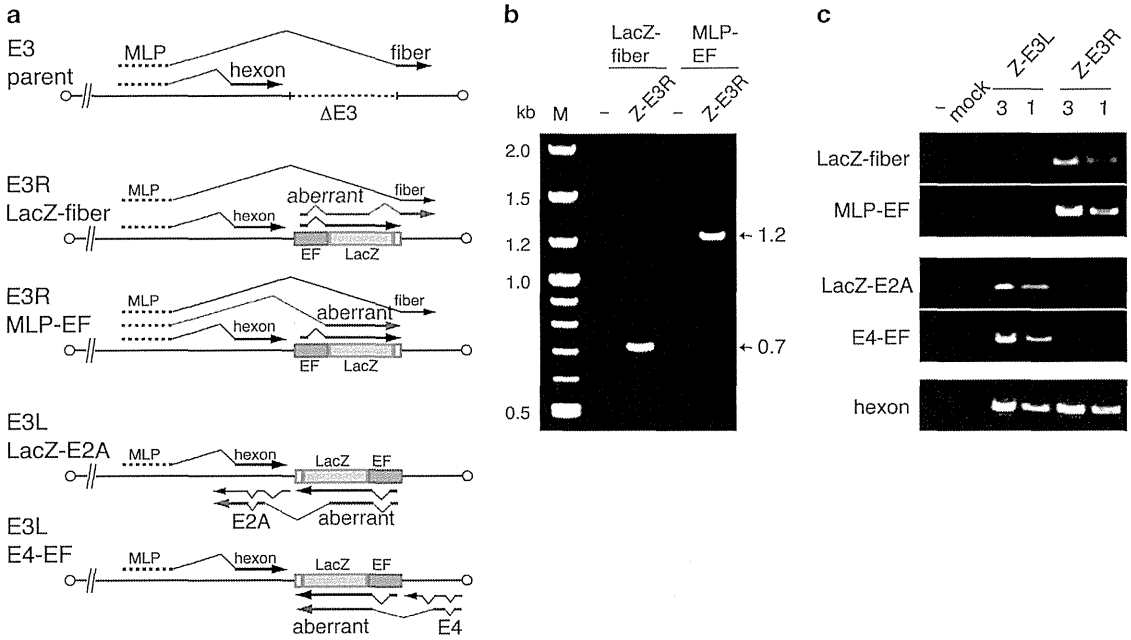

Figure 3. Structures of aberrant chimeric mRNAs. (**a**) Schematic representation of the aberrantly spliced mRNA and the expression unit in the E3 region. The LacZ expression units in the E3 region are shown. Aberrant mRNAs are shown in red. The bold lines and thin polygonal lines represent the exon and intron of the transcript, respectively. Arrow, orientation of the transcription; EF, EF1α promoter; LacZ, LacZ DNA. The 'parent' denotes the vectors before the insertion into the E3. 'LacZ-fiber,' 'MLP-EF,' 'LacZ-E2A' and 'E4-EF' indicate combinations of primers for detection of the chimeric mRNAs. (**b**) Detection of aberrant splicing by PCR. The 293 cells were infected with the Z-E3L and Z-E3R vectors, as indicated. The bands are generated from the chimera-specific mRNA between the viral gene and the inserted transgene. The primer sequences are shown in Supplementary Table S2. M, size maker; -, no DNA. (**c**) Specificity of the aberrant splicing. The 293 cells were infected with either Z-E3L or Z-E3R. The splicing from the MLP to hexon was used as the control. The bands of LacZ-fiber and MLP-EF in Z-E3R are the same as those described in (**b**) (0.7 and 1.2 kb, respectively). These bands were not detected in Z-E3L (lanes 3 and 1); threefold more DNA was loaded in lane 3 than in lane 1 to clearly show the semi-quantitative difference in the amount of cDNA. mock, mock infection of the 293 cells.

from the MLP donor to the EF1α acceptor and from LacZ donor to the fiber acceptor. We confirmed that these LacZ-fiber and MLP-EF aberrant mRNAs observed for the Z-E3R vector were not detected for the Z-E3L (Figure 3c, first and second rows).

We further examined whether such abnormal chimera mRNA was present for the Z-E3L vector of the opposite orientation. Actually, we detected two chimera mRNAs using the same PCR analysis; a viral E4 donor was spliced to the EF1α acceptor, and the

cryptic LacZ donor was spliced to a viral E2A acceptor (Figure 3a, fourth and fifth; Figure 3c, third and fourth rows. They were not detected for Z-E3R). The EF1α acceptor and LacZ donor were the same as those found in the E3L vector, and the sequences of the viral donor and the acceptor were identical to those found in the wild-type adenovirus, although the combinations were abnormal (Supplementary Table S1).

Then, we measured the amounts of fiber mRNA for the Z-E3R vector (very low titer) and compared them with those for the Z-E1L vector (high titer) and Z-E3L vector (medium titer) by conventional PCR and quantitative PCR (qPCR). These PCR and qPCR primers were designed to detect specifically the normal MLP-fiber mRNA, but not the aberrant mRNA, because they are prepared at the sequence junction: the forward and reverse primers are located in the MLP and fiber, respectively. The cDNAs from the 293 cells infected with Z-E1L, Z-E3L or Z-E3R were diluted from 10^0 to 10^{-3} before PCR (shown as '0' to '−3' in Figure 4a) for semi-quantitative detection (Figure 4a). The level of normal fiber mRNA of Z-E3L (middle titer) was lower and that of Z-E3R (very low titer) was much lower than that of Z-E1L (high titer), that is, the fiber mRNA levels and titers were well correlated. Notably, the amount of fiber mRNA of the Z-E3R vector was only 2% of that for the Z-E1L vector (Figure 4b, E3R). This may probably explain why the titer of Z-E3R was very low.

The expression of the E1 transgenes was higher than that of the E3 or E4 transgenes

The titers show amounts of infections virus particles produced by the vectors growing in the 293 cells, while expression levels are also important for the vector. The amounts of the produced gene products being influenced by the position of an identical expression unit on the cell chromosomes is referred to as the 'position effect' of gene expression.[13,14] To examine whether identical transgenes inserted into vector genomes are influenced or not by the 'position effect,' we infected the HuH-7 cells with the same numbers of active vector particles[16] expressing GFP under the control of the EF1α promoter at multiplicity of infection (MOI) 3 and 10 and measured the amounts of GFP mRNAs by qPCR (Figure 5a).

E1L and E1R vectors expressed much more GFP mRNA than the other three vectors, that is, the E3L, E4L and E4R vectors, both at MOI 3 and MOI 10 (bars 2 and 3 to 4, 6 and 7; bars 8 and 9 to 10, 12 and 13). In regard to the expression levels of these vectors, the mRNA amounts of the E4 vectors were about one-third of those of the E1 vectors. Similar results were obtained for the vectors expressing LacZ: E1L/R vectors expressed much more LacZ mRNA than all the E3 and E4 vectors, both at MOI 3 and MOI 10 (Figure 5b, bars 2 and 3 to 4–7; bars 8 and 9 to 10–13). Therefore, similar effects were observed using two different genes. These results might suggest that the position effect observed here was not dependent on the inserted transgene. It should be noted that about as much as a 50-fold more virus stock solution of Z-E3R vector could be needed than that of the Z-E1L vector to obtain the same expression level, because the titer of Z-E3R vector was about one-tenth and the expression level obtained was about one-fifth when the same volume of the virus stock solution is used for infection (Figure 2a, bars 7 and 10; Figure 5b, bars 2–5 and 8–11). We also measured the expressed protein levels of GFP and LacZ using fluorometry and β-galactosidase assay, respectively (Figure 6a and b). The G-E1 vectors produced significantly more GFP than the G-E4 vectors (Figure 6a, bars 2 and 3 to 6 and 7; bars 8 and 9 to 12 and 13), although the G-E3L vector expressed a similar level to that of the G-E1 vectors (bars 4 and 10). Also, the Z-E1 vectors expressed more LacZ than the Z-E3 and Z-E4 vectors (Figure 6b, bars 2 and 3 to 4–7; bars 8 and 9 to 10–13). These results in respect of the protein level confirm the mRNA expression levels measured by qPCR shown in Figure 5a and b.

To examine whether the position effects may also be observed for a tissue-specific promoter and for genes other than GFP and LacZ, the HuH-7 cells were infected with the vector expressing Cre under the control of the AFP promoter and the Cre expression levels were measured. The AFP promoter is specifically active in the HuH-7 cells derived from hepatocarcinoma in contrast to the case in the 293 cells. Because tissue-specific promoters, including the AFP promoter, are generally weak, the expressed Cre mRNA level was too low to measure quantitatively. Therefore, we used the method of 'excisional expression,' where the Cre enzyme driven by the AFP promoter switched on the potent EF1α promoter and specifically enhanced the expression level of dsRed by about 50-fold[17] (the strategy is shown in Supplementary Figure S1). The results were again very similar to those obtained using the EF1α promoter (Figure 6a and b): the AFP-E3 and E4 vectors expressed only about a half to one-fifth of dsRed mRNA than the AFP-E1 vectors (Figure 5c, bars 3 and 4 to 5–8, 9 and 10 to 11–14). Therefore, although the vector titers obtained using the AFP promoter were not influenced by their insertion sites (Figure 2b), the position effects at the E1, E3 and E4 sites showed very similar patterns to those of the EF1α promoter. Altogether, the E3L/R and E4L/R vectors expressed about two to fivefold less transgene products than the E1L/R vectors, not only when the potent EF1α promoter was used, but also when the tissue-specific AFP promoter was used, suggesting there may be a mechanism common to these promoters.

To examine whether the position effect of expression observed in the HuH-7 cells may also be observed in other cells, the HeLa cells were infected with the GFP-expressing vectors at MOI 3 and at MOI 10 (Figure 7a and b). The G-E1L vector expressed a significantly greater amount of mRNA than the G-E3 and G-E4 vectors (Figure 7a, bars 2 to 4, 6 and 7; bars 8 to 10, 12 and 13). However, the mRNA level of the E1R vector was not significantly different from those of the E3 and E4 vectors, because the

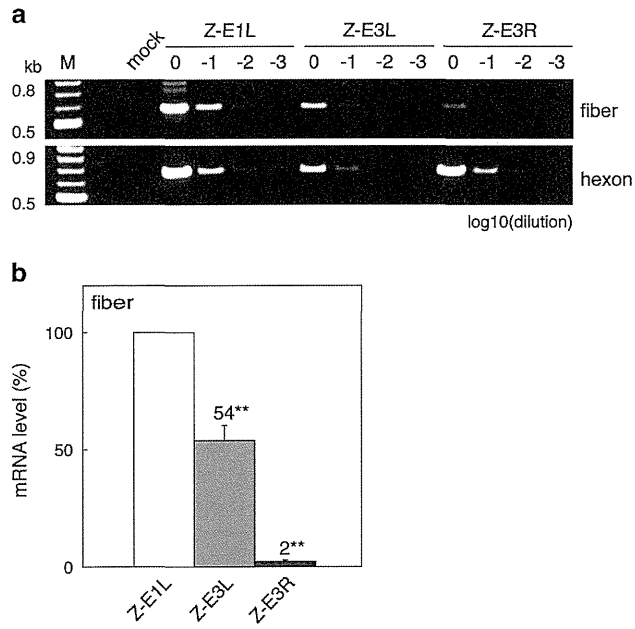

Figure 4. The relative levels of fiber mRNAs. The 293 cells were infected with the Z-E1L, Z-E3L and Z-E3R at MOI 5. (**a**) PCR detection of the fiber and hexon mRNAs. '0, -1, -2 and -3' mean '10^0, 10^{-1}, 10^{-2} and 10^{-3} dilution of the cDNAs', respectively. M, size marker; mock, mock infection of 293 cells. (**b**) The quantities of the fiber and hexon mRNAs determined by qPCR. Amount of fiber mRNA relative to those of each hexon and Z-E1L fiber are regarded as 100%. $n=3$; means ± s.d. ** $P<0.01$.

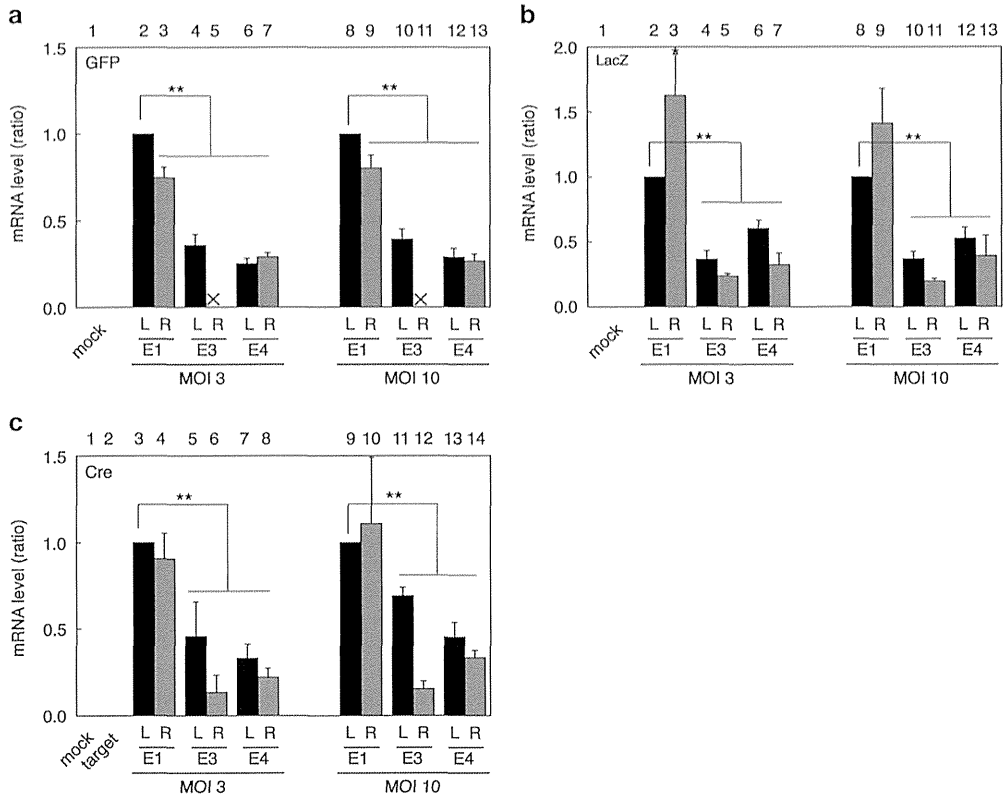

Figure 5. Expression levels of the transgene mRNA in the infected HuH-7 cells. The mRNA levels are shown relative to the mRNA level of the transgene in E1L-infected cells set as 1. (**a**) GFP mRNA levels. The cells were infected with the EF-GFP AdVs at the indicated MOIs. The GFP mRNA levels were quantified by qPCR, $n=3$. (**b**) LacZ mRNA levels. The cells were infected with the EF-LacZ AdVs. LacZ mRNA levels are shown in the same manner as that described in (**a**), $n=4$. (**c**) Cre mRNAs levels. The cells were co-infected with the AFP-Cre AdVs (switch vectors) and a target vector which expressed dsRed by Cre-mediated recombination (excisional expression). The dsRed mRNA levels were quantified in the same manner as that described in (**a**), $n=6$. Error bars indicate mean ± s.d; mock, HuH-7 cells without infection; target, HuH-7 cells infected with the target vector only; $^{*}P<0.05$, $^{**}P<0.01$. The other representations are the same as those in Figure 1.

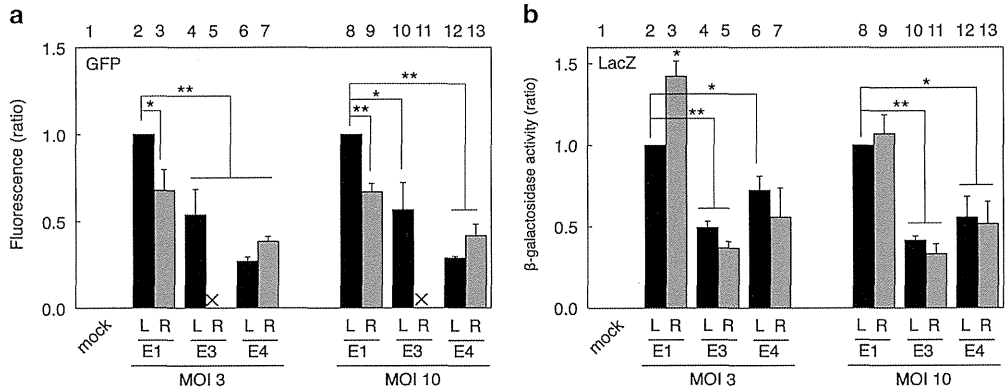

Figure 6. Protein expression levels in the infected HuH-7 cells. (**a**) Fluorescence of GFP. The cells were infected with the EF-GFP AdVs at the indicated MOIs. The fluorescence of GFP was quantified by Ascent fluorometry. The fluorescences are shown relative to the fluorescence level in E1L-infected cells set as 1, $n=4$. (**b**) Activities of β-galactosidase. The cells were infected with the EF-LacZ AdVs. β-galactosidase activities were evaluated by the β-gal assay, $n=3$. Error bars represent ± s.d.; mock, mock infection of HuH-7 cells; $^{*}P<0.05$, $^{**}P<0.01$. The other representations are the same as those in Figure 1.

expressed mRNA level of the E1R was lower than that of the E1L (bars 3 to 4, 6 and 7; bars 9 to 10, 12 and 13). Similar results were obtained using GFP fluorometry: the G-E1L vector exhibited significantly more fluorescence than the other G-E3 and G-E4 vectors (Figure 7b, bars 2 to 4, 6 and 7), whereas the E1R vector expression was not statistically significant (bars 3 to 4, 6 and 7). These results were confirmed by fluorescence microscopy (Supplementary Figure S2a). Moreover, the same results were obtained using the CV-1 cell line derived from monkey fibroblasts (Supplementary Figure S2b). Therefore, very similar position effect

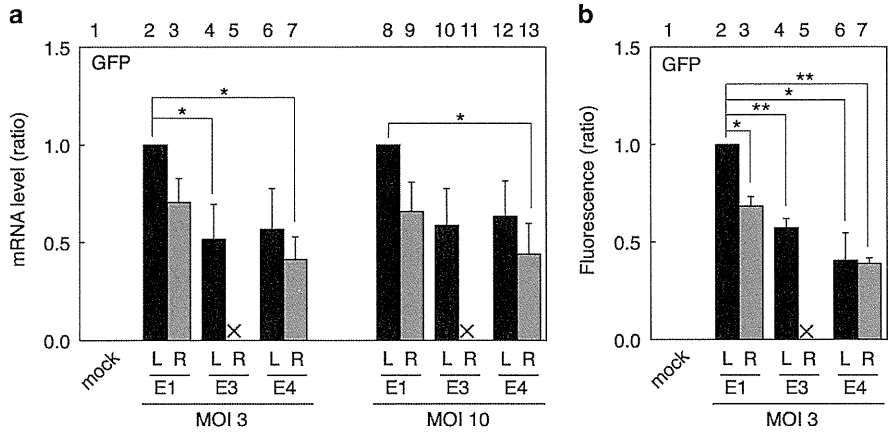

Figure 7. Expression levels of the transgene mRNA and protein in the infected HeLa cells. (**a**) GFP mRNA levels. The HeLa cells were infected with the EF-GFP AdVs at the indicated MOIs. The other representations are the same as those in Figure 4a, $n=3$. (**b**) Fluorescence of GFP. The HeLa cells were infected with EF-GFP AdVs at MOI 3. The other representations are the same as those in Figure 5a, $n=4$. Error bars indicate mean ± s.d.; mock, mock infection of HeLa cells; $*P<0.05$, $**P<0.01$.

among the E1, E3 and E4 insertion sites are obtained at least for the G-E1L vector.

DISCUSSION

We demonstrated in this study that the inserted sites and orientations for a given transgene greatly influenced the vector titers and expression levels. Especially, when the transgene was inserted in E3R, the GFP-expressing vector could not be obtained and the LacZ-expressing vector titer was extremely low. Also, the titer of E3L AdV was lower than that of E1L AdV. Because the aberrantly spliced mRNAs from the transgenes to a viral gene have been reported for the E1R site/orientation[15] (described below), and similar aberrant splicing might have occurred for E4L site/orientation in the same mechanism. Therefore, considering the titers, aberrant splicing and expression levels, E1L and E4R sites/orientations were preferable for the main target gene and the second gene, respectively, in the simultaneous expression. As for the titer, the information might be useful not only for FG AdVs but also for the replication-competent AdVs containing E1A gene under the control of a cancer-specific promoter, because they both are prepared using the 293 cells.

We have demonstrated that the vectors containing transgene at E1L/R showed higher titers and expression levels than other vectors. E1L/R is the most frequently used, probably because the E1 site is required or convenient for the major methods of AdV construction which are now commonly used.[18–20] For example, for the method established by the Graham's group, the use of the E1 site is essential because it exploits the viral packaging sequences partially overlapping with the E1 region. Consequently, we think that the E1 site, found to be the best in this work, might have been chosen in the currently popular methods. However, there seems to be one concern with E1R: aberrant splicing has been reported to occur to viral pIX gene from the cryptic donors present not only in the LacZ gene but also in the herpes thymidine-kinase (TK) gene, which is used for positron emission tomography as a reporter gene and for suicide gene therapy. Consequently, TK-pIX and LacZ-pIX fusion proteins were produced, and the pIX protein evokes strong immune responses.[15] For this reason, we always adopt the leftward orientation for the E1 site.

Currently, in the simultaneous expression of the target gene and the reporter gene, the E3 sites are mostly employed for the reporter gene.[21–25] However, as described here, when the LacZ-expressing transgene driven by the EF1α promoter was inserted at E3R, the vector titer and expression level were very low, probably because of the aberrant splicing, and the G-E3R AdV could not be obtained. In our experiences, the E3R AdV containing GFP gene driven by SRα promoter[26] could also not be obtained. In contrast, however, the E3R AdV containing GFP driven by CMV promoter could be obtained. The reason of such difference is unclear, but it might be related to the fact that both EF1α and SRα promoters contain the splicing unit including the splicing acceptor site in their promoters, which might produce the aberrant mRNA spliced from the MLP donor, but the CMV promoter contain no splicing unit. Because aberrant splicing was detected even at E3L, both E3R and E3L were problematic and to be avoided, if possible.

The E4 site has not frequently been used.[17,19,27–29] The E4 insertion position, *Sna*BI site, is located 162 nucleotides (nt) from the right end of the AdV genome. Vectors containing a transgene at the E4 site showed high titers, although their expression levels were lower than those of the E1 vectors. The titers and expression levels do not significantly differ between E4L and E4R vectors. However, the E4L might produce aberrantly spliced mRNAs as observed for the E3L/R. The E4R site/orientation was successfully used as the position of the second transgene[17] where Cre was expressed under the control of the AFP promoter. The expressed Cre turned on the potent promoter present at the E1L and the high-level expression of the target gene was obtained, while maintaining strict sepecificity. Interestingly, it was also recently reported that the E4L, not the E4R, is better than the E1 site for short hairpin RNA expression.[27] The difference may be related to the use of the RNA polymerase III promoter for the short hairpin RNA production, whereas the polymerase II promoter is used for the protein production. If so, the E4L may be advantageous not only for the production of short hairpin RNA, but also of guide RNAs used for the CRISPR/Cas9 system.[30,31] The reported results might not contradict with the results described here, because the RNA polymerase III expression is not involved with splicing.

Altogether, therefore, the E1L and E4R sites/orientations appear to be the best for use in AdVs for the simultaneous expression of the target gene and reporter gene, respectively. Importantly, the occurrence of aberrant splicing sometimes yields a viral-transgene fusion protein, which may induce strong immune responses caused by the viral encoding region.[15] The probability is one-third to coincide the coding frame of the transgene with that of the viral gene. The coding regions of the four aberrant mRNAs described in this report were, by chance, connected out-of-frame, yielding no transgene-fusion protein, but only a truncated LacZ protein composed of several amino acids. However, in a previous study,[15] LacZ-pIX and TK-pIX fusion proteins were produced under the control of potent promoters. Thus, the production of such fusion proteins by aberrant splicing is not a rare event.